ÉCOLE POLYTECHNIQUE FÉDÉRALE DE LAUSANNE

MATHICSE

Mathematics Institute of Computational Science and Engineering

School of Basic Sciences - Section of Mathematics

MATHICSE Technical Report

Nr. 18.2016

June 2016 (New 30.05.2017)

Efficient state/Parameter estimation in nonlinear unsteady PDEs by reduced basis ensemble Kalman filter

Stefano Pagani, Andrea Manzoni, Alfio Quarteroni

http://mathicse.epfl.ch

Address: EPFL - SB - MATHICSE (Bâtiment MA)
Station 8 - CH-1015 - Lausanne - Switzerland

Phone: +41 21 69 37648

Efficient State/Parameter Estimation in Nonlinear Unsteady PDEs by a Reduced Basis Ensemble Kalman Filter *

Stefano Pagani[‡] Andrea Manzoni[‡] Alfio Quarteroni[‡§]

May 30, 2017

Abstract

The ensemble Kalman filter is a computationally efficient technique to solve state and/or parameter estimation problems in the framework of statistical inversion when relying on a Bayesian paradigm. Unfortunately its cost may become moderately large for systems described by nonlinear time-dependent PDEs, because of the cost entailed by each PDE query. In this paper we propose a reduced basis ensemble Kalman filter technique to address the above problems. The reduction stage yields intrinsic approximation errors, whose propagation through the filtering process might affect the accuracy of state/parameter estimates. For an efficient evaluation of these errors, we equip our reduced basis ensemble Kalman filter with a reduction error model (or error surrogate). The latter is based on ordinary kriging for functional-valued data, to gauge the effect of state reduction on the whole filtering process. The accuracy and efficiency of the resulting method is then verified on the estimation of uncertain parameters for a FitzHugh-Nagumo model and uncertain fields for a Fisher-Kolmogorov model.

1 Introduction

The solution of backward uncertainty quantification (UQ) problems, for instance parameter estimation and statistical inverse problems, involving systems modeled by partial differential equations (PDEs) is computationally demanding. In this paper we develop an inversion technique that combines the reduced basis (RB) method and the ensemble Kalman filter (EnKF) for dynamical systems arising from the discretization of nonlinear time-dependent PDEs. The input parameter vector $\boldsymbol{\mu} \in \mathcal{P} \subset \mathbb{R}^d$ can characterize physical properties, geometrical quantities, boundary conditions, and forcing terms. In this context, we are interested to estimate the most likely value of $\boldsymbol{\mu}$ (in a sense to be made precise) by observing a set of noisy data (or measurements) $\mathbf{s} \in \mathbb{R}^s$. This latter involves an output $\mathbf{s}_h(\boldsymbol{\mu})$ provided by a linear functional of the PDE solution $\mathbf{u}_h(t;\boldsymbol{\mu})$ and an additive noise term. The pedix h typically refers to the gridsize of the numerical discretization; for small values of h, solving the estimation problem becomes computationally intensive. Following a Bayesian approach, both parameters $\boldsymbol{\mu}$ and outputs $\mathbf{s}$ are modeled as random vectors. In this setting, starting from the observation of the noisy data $\mathbf{s}$, the state/parameter estimation problem requires to characterize the posterior distribution of $[\boldsymbol{\mu}, \mathbf{u}_h]^T$. This latter is obtained by combining through the Bayes theorem the available a priori information on $\boldsymbol{\mu}$ and the likelihood function, depending on the output $\mathbf{s}_h$ (see e.g. [24, 34, 35]).

When the forward problem consists of a dynamical system, state/parameter estimation can be recast in the *Bayesian data assimilation* framework [21, 19]: the posterior distribution usually results from a sequential update which combines, at each step along the time interval, the knowledge on the estimated parameters until the current step, the measurements, and the output coming from the solution of the forward problem. Due to the nonlinearity of the input/output map $\boldsymbol{\mu} \to \mathbf{s}_h(\boldsymbol{\mu})$, the resulting posterior distribution cannot be written analytically. Its computation is typically

*This work was supported by the Italian National Group of Computing Science (GNCS-INDAM).

‡CMCS-MATH-SB, Ecole Polytechnique Fédérale de Lausanne, Station 8, CH-1015 Lausanne, Switzerland, {stefano.pagani,andrea.manzoni,alfio.quarteroni}@epfl.ch

§MOX, Dipartimento di Matematica, Politecnico di Milano, P.za Leonardo da Vinci 32, I-20133 Milano, Italy

based on sampling techniques, such as, e.g., sequential Monte Carlo methods, also referred to as *particle methods* [8].

In this paper we rely on the ensemble Kalman filter (EnKF), an ensemble-based data assimilation technique which combines the Kalman filter (KF) with a suitable sampling strategy. The EnKF sequentially produces an estimate of $[\boldsymbol{\mu}, \mathbf{u}_h]^T$ by a finite ensemble of vectors which are advanced in time according to the KF updating formula. Ensemble-based assimilation techniques are indeed well suited in situation where linearity and gaussianity assumptions are not matched. Since the EnKF also requires repetitive evaluations of solutions (and outputs) of the nonlinear dynamical system, solving a state/parameter estimation problem in this context still represents a computational challenge. The cost of the inversion procedure can be considerably reduced by approximating the dynamical system through surrogate or reduced order models (ROMs), see e.g. [2] for a survey of these techniques. In this work we exploit the RB method [31], relying on (i) the proper orthogonal decomposition (POD) technique for the basis construction and (ii) hyper-reduction techniques for the efficient evaluation of the nonlinear terms involved in the forward problem [26, 4, 30]. Recently a great effort has been devoted to the reduction of computational complexity entailed by inverse problems dealing with PDE system. For instance, ROMs have been exploited both within MCMC [15, 14, 27, 6, 20], and Bayesian filtering [32, 7] techniques to tackle state and/or parameter estimation problems.

With respect to already existing approaches, in this paper we develop for the first time a reduced basis ensemble Kalman filter (RB-EnKF) for the solution of state/parameter estimation problems governed by nonlinear time-dependent PDEs. A full-order (or high-fidelity) model (FOM) of the forward problem are typically based on finite elements, finite volumes or spectral methods. When a FOM is replaced by a ROM, the propagation of the approximation errors during the inversion procedure could lead to biased estimates of the unknown state/parameter [27, 22]. In order to enhance the accuracy of the estimation, we develop a statistical error model, to be included in the RB-EnKF to correct the bias on the output evaluation. Acting as a *calibration* of the reduced-order input/output map, this reduction error model (REM) can be obtained through a kriging interpolation procedure. This REM represents a possible extension of the ROM error surrogates proposed in [9, 27] in order to deal with nonlinear time-dependent problems, when cheap error bounds are not available.

To the best of our knowledge, this is the first investigation on the effect of the ROM on the accuracy of the filtering procedure. The ROM dimension can grow quite dramatically to ensure the achievement of a prescribed accuracy. Consequently, this entails a dramatic loss of computational efficiency. By equipping our RB-EnKF with a REM, we minimize the bias of state/parameter estimates when less accurate, but more efficient, ROMs are employed. This error analysis represents another original contribution of this paper: by adopting the perspective of functional data analysis, our REM is able to provide an efficient prediction of the propagation of the error on the estimated quantities.

The paper is organized as follows. In Section 2 we provide a general formulation of the class of problems we are interested to, whereas in Section 3 we introduce the EnKF, outlining the whole algorithm for state/parameter estimation. In Section 4 we exploit the RB method to solve nonlinear dynamical systems efficiently, and derive a RB formulation of the EnKF. Some theoretical results are also proven in order to carry out an a priori error analysis on the estimated quantities, with respect to the increasing accuracy of the underlying RB approximation. In Section 5 we introduce the kriging-based reduction error model, we incorporate it into the inversion procedure, and we provide an analysis of the estimation error with respect to the uncorrected RB-EnKF. In Section 6, we present some numerical results exploiting the proposed procedure for the estimation of unknown parameters or random fields when either a FitzHugh-Nagumo or a Fisher-Kolmogorov model is considered.

2 Problem formulation

In this section we introduce the class of problems we focus on, and recall some basic notions on the Bayesian approach instrumental to build the whole framework. For the sake of simplicity, we directly deal with the algebraic formulation of the *full-order model* (FOM), obtained by a finite

element approximation of the forward problem.

2.1 Forward problem

We consider as FOM the input/output map

$$\boldsymbol{\mu} \longmapsto \mathbf{s}_h(\boldsymbol{\mu}) = \int_0^T \mathbf{H}\mathbf{u}_h(t;\boldsymbol{\mu})dt \ \in \mathbb{R}^s, \tag{1}$$

where $\mathbf{u}_h = \mathbf{u}_h(t;\boldsymbol{\mu})$ is the solution of a nonlinear parametrized dynamical system, arising from the spatial semi-discretization of a nonlinear parabolic PDE:

$$\begin{cases} \mathbf{M}(\boldsymbol{\mu})\dfrac{\partial \mathbf{u}_h}{\partial t} + \mathbf{A}(\boldsymbol{\mu})\mathbf{u}_h + \mathbf{N}(\mathbf{u}_h;\boldsymbol{\mu}) = \mathbf{f}_h(t;\boldsymbol{\mu}), \qquad t \in (0,T) \\ \mathbf{u}_h(0;\boldsymbol{\mu}) = \mathbf{u}_0. \end{cases} \tag{2}$$

$\mathbf{H} \in \mathbb{R}^{s\times N_h}$ encodes the observation operator, $\mathbf{M}(\boldsymbol{\mu}) \in \mathbb{R}^{N_h\times N_h}$ the mass matrix, $\mathbf{f}_h \in \mathbb{R}^{N_h}$ the data of the PDE problem; $\mathbf{A}(\boldsymbol{\mu}) \in \mathbb{R}^{N_h\times N_h}$ and $\mathbf{N}(\cdot;\boldsymbol{\mu}) \in \mathbb{R}^{N_h}$ are a $\boldsymbol{\mu}$-dependent matrix and vector, respectively, encoding linear and nonlinear PDE operators. Note that $\boldsymbol{\mu}$ is constant over $(0,T)$, that is, it is not affected by state dynamics. Problem (2) arises e.g. by applying a Galerkin-finite element (FE) method using a finite-dimensional space $X_h \subset X$ of (possibly very large) dimension $\dim(X_h) = N_h$; $X = X(\Omega)$ denotes the functional space where the continuous problem is formulated, whereas $\Omega \in \mathbb{R}^p$, $p = 1, 2, 3$, is the spatial domain; h is a parameter related to the mesh size of the computational grid.

Given a partition $(t^{(\ell)}, t^{(\ell+1)})$, $\ell = 0, \dots, N_t - 1$ of $(0,T)$ into N_t subintervals of length Δt, we adopt the implicit Euler method for the time discretization, thus solving

$$\begin{cases} \left(\dfrac{\mathbf{M}(\boldsymbol{\mu})}{\Delta t} + \mathbf{A}(\boldsymbol{\mu})\right)\mathbf{u}_h^{(\ell+1)} + \mathbf{N}(\mathbf{u}_h^{(\ell+1)};\boldsymbol{\mu}) = \dfrac{\mathbf{M}(\boldsymbol{\mu})}{\Delta t}\mathbf{u}_h^{(\ell)} + \mathbf{f}_h^{(\ell+1)}(\boldsymbol{\mu}), \quad \ell = 0, \dots, N_t - 1 \\ \mathbf{u}_h^{(0)} = \mathbf{u}_0. \end{cases} \tag{3}$$

To solve the nonlinear problem in (3), we use the Newton method: at each time step $\ell = 1, \dots, N_t - 1$, while $\|\boldsymbol{\delta}_u^\imath\| < tol$, we solve

$$\mathbf{J}(\mathbf{u}_{h,\imath}^{(\ell+1)})\boldsymbol{\delta}_u^\imath = -\mathbf{r}(\mathbf{u}_{h,\imath}^{(\ell+1)}), \qquad \mathbf{u}_{h,\imath+1}^{(\ell+1)} = \mathbf{u}_{h,\imath}^{(\ell+1)} + \boldsymbol{\delta}_u^\imath \qquad \imath = 1, \dots, \tag{4}$$

with $\mathbf{u}_{h,0}^{(\ell+1)} = \mathbf{u}_h^{(\ell)}$ and $tol > 0$ a fixed small tolerance. The Jacobian matrix $\mathbf{J}$ and the residual vector $\mathbf{r}$ of the problem (2) are respectively given by

$$\begin{aligned} \mathbf{J}(\mathbf{v}) &= \frac{\mathbf{M}(\boldsymbol{\mu})}{\Delta t} + \mathbf{A}(\boldsymbol{\mu}) + \tilde{\mathbf{J}}(\mathbf{v};\boldsymbol{\mu}) \in \mathbb{R}^{N_h\times N_h}, \\ \mathbf{r}(\mathbf{v}) &= \frac{\mathbf{M}(\boldsymbol{\mu})}{\Delta t}(\mathbf{v} + \mathbf{u}_h^{(\ell)}) + \mathbf{A}(\boldsymbol{\mu})\mathbf{v} + \mathbf{N}(\mathbf{v};\boldsymbol{\mu}) - \mathbf{f}_h(t^{(\ell+1)};\boldsymbol{\mu}) \in \mathbb{R}^{N_h}; \end{aligned} \tag{5}$$

$\tilde{\mathbf{J}} \in \mathbb{R}^{N_h\times N_h}$ is the Jacobian matrix of the nonlinear term $\mathbf{N}$.

Since the state/parameter estimation problem is performed sequentially over the time interval $(0,T)$, we need to evaluate the input/output map (1) at various time steps instead than only once. We introduce a coarse partition of the time interval $(0,T)$ into N_τ windows $(\tau^{(k)}, \tau^{(k+1)})$ of length $\Delta\tau = K\Delta t$, with $k = 0, \dots, N_\tau - 1$ and $K > 1$ (a sketch is reported in Fig. 1). Therefore, we consider as outputs over each window $(\tau^{(k)}, \tau^{(k+1)})$ the values

$$\mathbf{s}_h^{(k+1)}(\boldsymbol{\mu}) = \int_{\tau^{(k)}}^{\tau^{(k+1)}} \mathbf{H}\mathbf{u}_h(t;\boldsymbol{\mu})dt \approx \Delta t\mathbf{H}\sum_{\ell=Kk}^{K(k+1)} \omega_\ell \mathbf{u}_h(t^{(\ell)};\boldsymbol{\mu}), \qquad k = 0, \dots, N_\tau - 1, \tag{6}$$

where ω_ℓ, $\ell = Kk, \dots, K(k+1)$ are weights depending on the chosen quadrature formula.

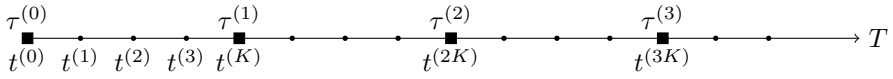

Figure 1: Example of partition of the time interval in windows of length $\Delta\tau = K\Delta t$, $K = 4$

Remark 1. *For the numerical experiments discussed in this paper, we consider data coming from a particular (noisy) realizations of the FOM; hence, we assume that data are available at each time step $t^{(k)}$, $k = 1, \dots, N_t$. Choosing the outputs as in* (6) *then reflects the availability of $K > 1$ observations on each assimilation window $(\tau^{(k)}, \tau^{(k+1)})$. A possible alternative – more closely related to real measurements of observational data, acquired with a given time frequency – would be to consider as outputs the measured values at each $t = \tau^{(k+1)}$, i.e. $\mathbf{s}_h^{(k+1)}(\boldsymbol{\mu}) = \mathbf{H}\mathbf{u}_h(\tau^{(k+1)}; \boldsymbol{\mu})$, $k = 0, \dots, N_\tau - 1$; definition* (6) *however does not impact on the formulation of the proposed methodology, this latter being independent of the particular output choice.*

2.2 Bayesian data assimilation

We formulate the problem of estimating $\boldsymbol{\mu} \in \mathcal{P} \subset \mathbb{R}^d$ and $\mathbf{u}_h \in X_h$ from noisy data $\{\mathbf{s}^{(k)}\}_{k=1}^{N_\tau} \in \mathbb{R}^{N_\tau \times s}$ as a Bayesian data assimilation problem. Following the approach proposed in [1, 19], the solution of this problem at iteration $k = 1, \dots, N_\tau$, is given by a multivariate probability density function (pdf) $\pi_{post} : \mathcal{P} \times X_h \to \mathbb{R}_0^+$ of the parameters $\boldsymbol{\mu}$ and the state $\mathbf{u}_h$ given the noisy data $\mathcal{S}^{(k)} = \{\mathbf{s}^{(i)}\}_{i=1}^k$. Thanks to the *Bayes theorem*, we can express π_{post} as

$$\pi_{post}\left([\boldsymbol{\mu}, \mathbf{u}_h^{(k)}]^T \;\middle|\; \mathcal{S}^{(k)} \right) = \frac{1}{\eta(\mathbf{s})} \pi\left(\mathcal{S}^{(k)} \;\middle|\; [\boldsymbol{\mu}, \mathbf{u}_h^{(k)}]^T \right) \pi_{\text{prior}}\left([\boldsymbol{\mu}, \mathbf{u}_h^{(k)}]^T \right), \tag{7}$$

where $\pi_{\text{prior}} : \mathcal{P} \times X_h \to \mathbb{R}_0^+$ is the *prior* pdf of the parameters/state vector, $\pi : \mathbb{R}^{k \times s} \to \mathbb{R}_0^+$ the *likelihood* function and $\eta(\mathbf{s})$ a suitable normalization constant, which does not affect the inversion step [35, 25]. We consider an additive noise model: given $\boldsymbol{\mu} = \boldsymbol{\mu}^*$, set

$$\mathbf{s}^{(k)} = \mathbf{s}_h^{(k)}(\boldsymbol{\mu}^*) + \boldsymbol{\varepsilon}_{\text{noise}} \qquad \forall k = 1, \dots, N_\tau \tag{8}$$

where we assume that the noise is independent from a time step to another and is modeled by a gaussian random variable $\boldsymbol{\varepsilon}_{\text{noise}} \sim \mathcal{N}(\mathbf{0}, \boldsymbol{\Gamma})$, with covariance matrix $\Gamma \in \mathbb{R}^{s \times s}$. Under these assumptions, the likelihood function can be expressed as:

$$\pi\left(\mathcal{S}^{(k)} \;\middle|\; [\boldsymbol{\mu}, \mathbf{u}_h^{(k)}]^T \right) = \pi\left(\mathbf{s}^{(k)} \;\middle|\; [\boldsymbol{\mu}, \mathbf{u}_h^{(k)}]^T \right) \pi\left(\mathcal{S}^{(k-1)} \;\middle|\; [\boldsymbol{\mu}, \mathbf{u}_h^{(k)}]^T \right),$$

and, consequently, (7)

$$\begin{aligned} \pi_{post}\left([\boldsymbol{\mu}, \mathbf{u}_h^{(k)}]^T \;\middle|\; \mathcal{S}^{(k)} \right) &= \frac{1}{\eta(\mathbf{s})} \pi\left(\mathbf{s}^{(k)} \;\middle|\; [\boldsymbol{\mu}, \mathbf{u}_h^{(k)}]^T \right) \pi\left(\mathcal{S}^{(k-1)} \;\middle|\; [\boldsymbol{\mu}, \mathbf{u}_h^{(k)}]^T \right) \pi_{\text{prior}}\left([\boldsymbol{\mu}, \mathbf{u}_h^{(k)}]^T \right) \\ &= \frac{1}{\eta(\mathbf{s})} \pi\left(\mathbf{s}^{(k)} \;\middle|\; [\boldsymbol{\mu}, \mathbf{u}_h^{(k)}]^T \right) \pi_{post}\left([\boldsymbol{\mu}, \mathbf{u}_h^{(k)}]^T \;\middle|\; \mathcal{S}^{(k-1)} \right). \end{aligned} \tag{9}$$

Equation (9) expresses the sequential updating of the posterior pdf of $[\boldsymbol{\mu}, \mathbf{u}_h]^T$ given the measurement vectors $\mathcal{S}^{(k)}$. Under the assumption that $\boldsymbol{\varepsilon}_{\text{noise}}$ is normally distributed, we have that

$$\pi\left(\mathbf{s}^{(k)} \middle| [\boldsymbol{\mu}, \mathbf{u}_h^{(k)}]^T \right) = \frac{1}{(2\pi)^{(\frac{s}{2})} |\Gamma|^{\frac{1}{2}}} \exp\left\{ -\frac{1}{2} \|\mathbf{s}^{(k)} - \mathbf{s}_h^{(k)}(\boldsymbol{\mu})\|_{\boldsymbol{\Gamma}}^2 \right\}, \tag{10}$$

where the weighted norm $\|\cdot\|_{\boldsymbol{\Gamma}}$ is such that $\|\mathbf{v}\|_{\boldsymbol{\Gamma}}^2 = \mathbf{v}^T \Gamma^{-1} \mathbf{v}$, $\mathbf{v} \in \mathbb{R}^s$.
The estimated parameter values evolve along the simulation period, and the actual estimation is achieved with the final values, that is, $\pi_{post}([\boldsymbol{\mu}, \mathbf{u}_h^{(N_\tau)}]^T \mid \mathcal{S}^{(N_\tau)})$ provides the solution of the estimation problem.

The EnKF takes advantage of a randomly generated sample to successively update the distribution of interest $\pi_{post}([\boldsymbol{\mu}, \mathbf{u}_h^{(k)}]^T | \mathcal{S}^{(k)})$ in an efficient way. For the sake of notation we will use the

shorthand $\pi^{(k)}$ and $\pi^{(k)}_{post}$ to denote $\pi(\mathbf{s}^{(k)}|[\boldsymbol{\mu}, \mathbf{u}_h^{(k)}]^T)$ and $\pi_{post}([\boldsymbol{\mu}, \mathbf{u}_h^{(k)}]^T|\mathcal{S}^{(k)})$, respectively. In the following section we recall the basic features of this technique, a more detailed overview can be found e.g. in [12, 23].

3 Ensemble Kalman filter

The EnKF is a recursive filter widely exploited in Bayesian data assimilation and forecasting, see e.g. [11, 21, 19]. It is based on the updating of a particles *ensemble* using the prediction/analysis procedure introduced in the previous section. In our case, by particle *ensemble* we mean a sample of N_e parameter vectors

$$\mathcal{P}_h^{(k)} = \{\boldsymbol{\mu}_{h,q}^{(k)}\}_{q=1}^{N_e}, \qquad k = 1, \dots, N_\tau,$$

where $\boldsymbol{\mu}_{h,q}^{(k)}$ denotes the value of a parameter vector $\boldsymbol{\mu}_{h,q}$ at the $k-th$ iteration, and the associated ensemble of N_e state solutions

$$\mathcal{U}_h^{(k)} = \{\mathbf{u}_h^{(k)}(\boldsymbol{\mu}),\ \boldsymbol{\mu} \in \mathcal{P}_h^{(k)}\}, \qquad k = 1, \dots, N_\tau.$$

Moreover, let us introduce, for any $k = 1, \dots, N_\tau$, the sample mean vectors

$$\overline{\mathbf{u}}_h^{(k)} = \frac{1}{N_e} \sum_{\boldsymbol{\mu} \in \mathcal{P}_h^{(k-1)}} \mathbf{u}_h^{(k)}(\boldsymbol{\mu}), \qquad \overline{\mathbf{s}}_h^{(k)} = \frac{1}{N_e} \sum_{\boldsymbol{\mu} \in \mathcal{P}_h^{(k-1)}} \mathbf{s}_h^{(k)}(\boldsymbol{\mu}), \qquad \overline{\boldsymbol{\mu}}_h^{(k)} = \frac{1}{N_e} \sum_{\boldsymbol{\mu} \in \mathcal{P}_h^{(k)}} \boldsymbol{\mu}, \tag{11}$$

the sample covariance of the outputs

$$\mathbf{C}_{s_h s_h}^{(k)} = \frac{1}{N_e - 1} \sum_{\boldsymbol{\mu} \in \mathcal{P}_h^{(k-1)}} (\mathbf{s}_h^{(k)}(\boldsymbol{\mu}) - \overline{\mathbf{s}}_h^{(k)})(\mathbf{s}_h^{(k)}(\boldsymbol{\mu}) - \overline{\mathbf{s}}_h^{(k)})^T \in \mathbb{R}^{s \times s} \tag{12}$$

and the sample cross-covariances

$$\mathbf{C}_{\mu_h s_h}^{(k)} = \frac{1}{N_e - 1} \sum_{\boldsymbol{\mu} \in \mathcal{P}_h^{(k-1)}} (\boldsymbol{\mu} - \overline{\boldsymbol{\mu}}^{(k-1)})(\mathbf{s}_h^{(k)}(\boldsymbol{\mu}) - \overline{\mathbf{s}}_h^{(k)})^T \in \mathbb{R}^{d \times s}, \tag{13}$$

$$\mathbf{C}_{u_h s_h}^{(k)} = \frac{1}{N_e - 1} \sum_{\boldsymbol{\mu} \in \mathcal{P}_h^{(k-1)}} (\mathbf{u}_h^{(k)}(\boldsymbol{\mu}) - \overline{\mathbf{u}}_h^{(k)})(\mathbf{s}_h^{(k)}(\boldsymbol{\mu}) - \overline{\mathbf{s}}_h^{(k)})^T \in \mathbb{R}^{N_h \times s}. \tag{14}$$

Starting from the initial ensemble $\{\mathcal{P}_h^{(0)}, \mathcal{U}_h^{(0)}\}$ sampled from the prior distribution, and the given data $\mathbf{s}^{(k)}$, $k = 1, \dots, N_\tau$, the *prediction-analysis* procedure of the EnKF is given by the following two stages recursion:

1. *prediction stage*:
   - compute the solution $\mathbf{u}_h^{(k+1)}(\boldsymbol{\mu})$ of the forward problem (3) over $[\tau^{(k)}, \tau^{(k+1)})$ with initial datum $\mathbf{u}_h^{(k)}(\boldsymbol{\mu}) \in \mathcal{U}^{(k)}$, and the output $\mathbf{s}_h^{(k+1)}(\boldsymbol{\mu})$ for each $\boldsymbol{\mu} \in \mathcal{P}_h^{(k)}$;
   - compute the sample means $\overline{\mathbf{u}}_h^{(k+1)}$, $\overline{\mathbf{s}}_h^{(k+1)}$ and $\overline{\boldsymbol{\mu}}^{(k)}$;
   - compute the sample covariance $\mathbf{C}_{s_h s_h}^{(k+1)}$ and cross-covariances $\mathbf{C}_{\mu_h s_h}^{(k+1)}$, $\mathbf{C}_{u_h s_h}^{(k+1)}$.
2. *analysis stage*: update the state/parameter ensemble by taking advantage of the new information from the prediction stage, through the following *KF updating formula*:

$$\begin{bmatrix} \boldsymbol{\mu}_{h,q}^{(k+1)} \\ \mathbf{u}_h^{(k+1)}(\boldsymbol{\mu}_{h,q}^{(k+1)}) \end{bmatrix} = \begin{bmatrix} \boldsymbol{\mu}_{h,q}^{(k)} \\ \mathbf{u}_h^{(k+1)}(\boldsymbol{\mu}_{h,q}^{(k)}) \end{bmatrix} + \begin{bmatrix} \mathbf{C}_{\mu_h s_h}^{(k+1)} \\ \mathbf{C}_{u_h s_h}^{(k+1)} \end{bmatrix} (\boldsymbol{\Gamma} + \mathbf{C}_{s_h s_h}^{(k+1)})^{-1} (\mathbf{s}_q^{(k+1)} - \mathbf{s}_h^{(k+1)}(\boldsymbol{\mu}_{h,q}^{(k)})), \tag{15}$$

   for each $q = 1, \dots, N_e$, where N_e realizations of the noise $\boldsymbol{\varepsilon}_q^{(k+1)}$, $q = 1, \dots, N_e$, are added to the data to generate $\mathbf{s}_q^{(k+1)} = \mathbf{s}_h^{(k+1)}(\boldsymbol{\mu}^*) + \boldsymbol{\varepsilon}_q^{(k+1)}$.

At each iteration we estimate $\boldsymbol{\mu}^*$ through the sample mean $\hat{\boldsymbol{\mu}}_h = \overline{\boldsymbol{\mu}}_h$, and compute an empirical confidence region from the updated ensemble $\mathcal{P}_h^{(k+1)}$. For further properties of the EnKF see, e.g., [3, 10]. A detailed description of the procedure is reported in Algorithm 1.

Algorithm 1 Full-order Ensemble Kalman filter procedure

procedure EnKF
  Initialization:
  $\{\mathcal{P}_h^{(0)}, \mathcal{U}_h^{(0)}\} \leftarrow$ sampling N_e particles from π_{prior}
  for $q = 1 : N_e$, $k = 1 : N_\tau$ **do**
    $\mathbf{s}_q^{(k)} \leftarrow \mathbf{s}_h^{(k)}(\boldsymbol{\mu}^*) + \boldsymbol{\varepsilon}_q^{(k)}$
  end for
    Prediction/analysis stage:
    for $k = 0 : N_\tau - 1$ **do**
      Prediction stage:
      for $[\boldsymbol{\mu}, \mathbf{u}_h^{(k)}(\boldsymbol{\mu})]^T \in \{\mathcal{P}_h^{(k)}, \mathcal{U}_h^{(k)}\}$ **do**
        $\mathbf{u}_h^{(k+1)}(\boldsymbol{\mu}) \leftarrow$ solve forward problem (3) with initial datum $\mathbf{u}_h^{(k)}(\boldsymbol{\mu})$
      end for
       compute means $\overline{\mathbf{u}}_h^{(k+1)}, \overline{\mathbf{s}}_h^{(k+1)}$, and $\overline{\boldsymbol{\mu}}_h^{(k)}$ by (11)
       compute (cross-)covariances $\mathbf{C}_{s_h s_h}^{(k+1)}$ by (12), $\mathbf{C}_{u_h s_h}^{(k+1)}$ and $\mathbf{C}_{\mu_h s_h}^{(k+1)}$ by (13)
      Analysis stage:
      for $[\boldsymbol{\mu}] \in \{\mathcal{P}_h^{(k)}\}$ **do**
        update each state/parameter particle using (15)
      end for
    end for
  end procedure

4 Reduced-order model

Even if at each step $k = 1, \dots,$ the sequential update through the EnKF requires solving the forward problem on $[\tau^{(k)}, \tau^{(k+1)})$ for each particle in the ensemble, entailing severe computational costs. The nonlinear nature of the forward problem makes the whole estimation process even more challenging. For a fast evaluation of the *prediction* stage, we take advantage of the RB method, which we sketch below.

4.1 Reduced basis method

The RB method is a projection-based ROM which computes an approximation $\mathbf{u}_n(t;\boldsymbol{\mu})$ of $\mathbf{u}_h(t;\boldsymbol{\mu})$ (as well as an approximation $\mathbf{s}_n(\boldsymbol{\mu})$ of the output $\mathbf{s}_h(\boldsymbol{\mu})$) by means of a Galerkin projection on a reduced subspace $X_n \subset X_h$ of very small dimension $n \ll N_h$ (see e.g. [31] for a detailed overview). Here we construct such a space by means of the POD technique. This latter selects as basis functions the first n singular vectors (corresponding to the largest n singular values) of the snapshot matrix, whose columns are given by the full-order solution $\mathbf{u}_h(t^{(\ell)};\boldsymbol{\mu}_j)$, computed for each time-step $t^{(\ell)}$, $\ell = 1, \dots, N_t$ and a sufficiently rich sample $S_{train} = \{\boldsymbol{\mu}_1, \dots, \boldsymbol{\mu}_{N_{train}}\}$ of the parameter space $\mathcal{P} \subset \mathbb{R}^d$. S_{train} is built by drawing random samples from a uniform distribution whose support is $\mathcal{P}$; alternative techniques, such as latin hypercube sampling, can also be employed. Given the matrix $\mathbf{V} \in \mathbb{R}^{N_h \times n}$ which collects the basis functions, we approximate the full-order solution as $\mathbf{u}_h(t;\boldsymbol{\mu}) \approx \mathbf{V}\mathbf{u}_n$. The RB dimension n is chosen so that $\|\mathbf{u}_h(t;\boldsymbol{\mu}) - \mathbf{V}\mathbf{u}_n(t;\boldsymbol{\mu})\|_{X_h} < \epsilon_{tol}$ for each $\boldsymbol{\mu} \in S_{train}$, $t \in (0,T)$ and a given tolerance $\epsilon_{tol} > 0$. By projecting (2) onto the space generated by the columns of $\mathbf{V} \in \mathbb{R}^{N_h \times n}$ we compute $\mathbf{u}_n(t;\boldsymbol{\mu}) \in \mathbb{R}^n$ as the solution of the following reduced nonlinear parametrized dynamical system:

$$\begin{cases} \mathbf{M}_n(\boldsymbol{\mu})\dfrac{\partial \mathbf{u}_n}{\partial t} + \mathbf{A}_n(\boldsymbol{\mu})\mathbf{u}_n + \mathbf{V}^T\mathbf{N}(\mathbf{V}\mathbf{u}_n;\boldsymbol{\mu}) = \mathbf{f}_n(t;\boldsymbol{\mu}), \qquad t \in (0,T) \\ \mathbf{u}_n(0;\boldsymbol{\mu}) = \mathbf{V}^T\mathbf{u}_0 \end{cases} \tag{16}$$

where $\mathbf{M}_n(\boldsymbol{\mu}) = \mathbf{V}^T\mathbf{M}(\boldsymbol{\mu})\mathbf{V}$, $\mathbf{A}_n(\boldsymbol{\mu}) = \mathbf{V}^T\mathbf{A}(\boldsymbol{\mu})\mathbf{V}$ and $\mathbf{f}_n(t;\boldsymbol{\mu}) = \mathbf{V}^T\mathbf{f}_h(t;\boldsymbol{\mu})$.

Proceeding similarly to the full-order case concerning time discretization, the implicit Euler method applied to (16) yields the following dynamical system:

$$\begin{cases} \left(\dfrac{\mathbf{M}_n(\boldsymbol{\mu})}{\Delta t} + \mathbf{A}_n(\boldsymbol{\mu})\right)\mathbf{u}_n^{(\ell+1)} + \mathbf{V}^T\mathbf{N}(\mathbf{V}\mathbf{u}_n^{(\ell+1)};\boldsymbol{\mu}) \\ \qquad\qquad = \dfrac{\mathbf{M}_n(\boldsymbol{\mu})}{\Delta t}\mathbf{u}_n^{(\ell)} + \mathbf{f}_n(t^{(\ell+1)};\boldsymbol{\mu}), \qquad \ell = 0,\dots,N_t-1 \\ \mathbf{u}_n^{(0)} = \mathbf{V}^T\mathbf{u}_0. \end{cases} \tag{17}$$

Due to the presence of the nonlinear term $\mathbf{N}(\cdot;\boldsymbol{\mu})$, we use the Newton method as follows: while $\|\boldsymbol{\delta}_{u_n}^{\imath}\| < tol$, we solve

$$\mathbf{J}_n(\mathbf{u}_{n,\imath}^{(\ell+1)})\boldsymbol{\delta}_{u_n}^{\imath} = -\mathbf{r}_n(\mathbf{u}_{n,\imath}^{(\ell+1)}), \qquad \mathbf{u}_{n,\imath+1}^{(\ell+1)} = \mathbf{u}_{n,\imath}^{(\ell+1)} + \boldsymbol{\delta}_u^{\imath} \qquad \imath = 1,\dots, \tag{18}$$

with $\mathbf{u}_{n,0}^{(\ell+1)} = \mathbf{u}_n^{(\ell)}$. The reduced Jacobian matrix $\mathbf{J}_n \in \mathbb{R}^{n\times n}$ and the reduced residual vector $\mathbf{r}_n \in \mathbb{R}^n$ of the problem (17) are

$$\mathbf{J}_n(\mathbf{v}) = \frac{\mathbf{M}_n(\boldsymbol{\mu})}{\Delta t} + \mathbf{A}_n(\boldsymbol{\mu}) + \mathbf{V}^T\tilde{\mathbf{J}}(\mathbf{V}\mathbf{v};\boldsymbol{\mu}) \in \mathbb{R}^{n\times n}, \qquad \mathbf{v}\in\mathbb{R}^n,$$

and

$$\mathbf{r}_n(\mathbf{v}) = \frac{\mathbf{M}_n(\boldsymbol{\mu})}{\Delta t}(\mathbf{v}+\mathbf{u}_n^{(\ell)}) + \mathbf{A}_n(\boldsymbol{\mu})\mathbf{v} + \mathbf{V}^T\mathbf{J}_N(\mathbf{V}\mathbf{v};\boldsymbol{\mu}) - \mathbf{f}_n(t^{(\ell+1)};\boldsymbol{\mu}) \in \mathbb{R}^n,$$

respectively. For the ROM output evaluation, we consider the integral of the reduced output vector over each interval $(\tau^{(k)},\tau^{(k+1)}]$, that is

$$\mathbf{s}_n^{(k+1)}(\boldsymbol{\mu}) = \int_{\tau^{(k)}}^{\tau^{(k+1)}} \mathbf{H}_n\mathbf{u}_n(t;\boldsymbol{\mu})dt, \qquad \forall k = 0,\dots,N_\tau-1,$$

where the reduced output operator is defined as $\mathbf{H}_n = \mathbf{H}\mathbf{V} \in \mathbb{R}^{s\times n}$. As a consequence, the additive noise model (8) is now replaced by

$$\mathbf{s}^{(k)} = \mathbf{s}_n^{(k)}(\boldsymbol{\mu}^*) + \boldsymbol{\varepsilon}_{\text{noise}}, \qquad \forall k = 1,\dots,N_\tau.$$

The efficient evaluation of the reduced arrays appearing in (17) as time and parameters vary is still a challenging task in order to achieve an efficient online evaluation of a ROM when dealing with nonlinear (and/or complex nonaffine) terms. Indeed, under the assumption of *affine parametric dependence*, those arrays can be expressed as the finite sum of products between $\boldsymbol{\mu}$-dependent functions and $\boldsymbol{\mu}$-independent operators [31]. In nonaffine cases, an (approximate) affine approximation can be recovered by means of the *empirical interpolation method* (EIM), see e.g. [26]. For instance, given a nonaffine operator $\mathbf{A}(\boldsymbol{\mu})$, the EIM approximation reads

$$\mathbf{A}(\boldsymbol{\mu}) \approx \sum_{j=1}^{m_{\text{EIM}}} \beta_j(\boldsymbol{\mu})\mathbf{A}^j$$

where for any $\boldsymbol{\mu}\in\mathcal{P}$, the coefficients $\{\beta_j(\boldsymbol{\mu})\}_{j=1}^{m_{\text{EIM}}}$ are evaluated by solving a linear system of dimension $m_{\text{EIM}}\times m_{\text{EIM}}$, arising by the imposition of m_{EIM} interpolation constraints over a set of m_{EIM} magic points selected according to a suitable greedy procedure (see [26]). Given this approximation, the reduced operator can then be obtained as

$$\mathbf{A}_n(\boldsymbol{\mu}) = \sum_{k=1}^{m_{\text{EIM}}} \beta_j(\boldsymbol{\mu})\mathbf{A}_n^j, \qquad \mathbf{A}_n^j = \mathbf{V}^T\mathbf{A}^j\mathbf{V}.$$

In this way, computations can be decoupled into an expensive $\boldsymbol{\mu}$-independent *offline* stage and a very inexpensive $\boldsymbol{\mu}$-dependent *online* stage, to be performed several times during the inversion algorithm. Unfortunately, when dealing with nonlinear operators, evaluating $\mathbf{V}^T\mathbf{N}(\mathbf{V}\cdot;\boldsymbol{\mu})$ would also depend on the FOM size N_h, and therefore still very expensive. To overcome this problem, the *(discrete) empirical interpolation method* (DEIM) can be exploited at each iteration of the Newton

algorithm to handle the $\boldsymbol{\mu}$-dependent nonlinear terms efficiently, as proposed in [4] and further discussed in [30]. In particular, the DEIM approximation of a nonlinear operator $\mathbf{N} : \mathbb{R}^{N_h} \to \mathbb{R}^{N_h}$ is given by

$$\mathbf{N}(\mathbf{V}\mathbf{u}_n; \boldsymbol{\mu}) \approx \sum_{j=1}^{m_D} c_j(\mathbf{u}_h; \boldsymbol{\mu})\phi_j(\mathbf{x}), \tag{19}$$

where the coefficients $\{c_j\}_{k=1}^{m_\mathrm{D}}$ can be computed at each iteration by solving a $m_\mathrm{D} \times m_\mathrm{D}$ linear system. In particular, by defining the basis matrix $\mathbf{U} = [\phi_1, \ldots, \phi_{m_\mathrm{D}}]$ and the index matrix $P = [\mathbf{e}_{i1}, \ldots, \mathbf{e}_{im_\mathrm{D}}]$, we get the following reduced approximation of the nonlinear function

$$\mathbf{V}^T\mathbf{N}(\mathbf{V}\mathbf{u}_n; \boldsymbol{\mu}) \approx \underbrace{\mathbf{V}^T\mathbf{U}(\mathbf{P}^T\mathbf{U})^{-1}}_{n\times m_\mathrm{D}} \underbrace{\mathbf{N}(\mathbf{P}^T\mathbf{V}\mathbf{u}_n; \boldsymbol{\mu})}_{m_\mathrm{D}\times 1} \in \mathbf{R}^n.$$

In the case of the implicit Euler method, also the Jacobian $\mathbf{J}_N$ has to be assembled efficiently at each Newton step. For the case at hand, we can directly differentiate (19), yielding

$$\mathbf{V}^T\tilde{\mathbf{J}}(\mathbf{V}\mathbf{u}_n; \boldsymbol{\mu}) \approx \underbrace{\mathbf{V}^T\mathbf{U}(\mathbf{P}^T\mathbf{U})^{-1}}_{n\times m_\mathrm{D}} \underbrace{\mathbf{J}_N(\mathbf{P}^T\mathbf{V}\mathbf{u}_n; \boldsymbol{\mu})}_{m_\mathrm{D}\times m_\mathrm{D}} \underbrace{\mathbf{P}^T\mathbf{V}}_{m_\mathrm{D}\times n} \in \mathbf{R}^{n\times n}.$$

Alternative solutions can be obtained by considering an extension of DEIM for sparse Jacobians, known as *matrix* DEIM; see also the related discussion in [30, 33].

4.2 Reduced basis Ensemble Kalman filter

Given a suitable ROM to solve the forward problem, a reduced-order EnKF can be obtained by replacing the full-order output evaluation with the reduced-order one. Since we have adopted the RB method, we will refer to the resulting procedure as to RB-EnKF. We define the ensemble of N_e parameters as

$$\mathcal{P}_n^{(k)} = \{\boldsymbol{\mu}_{n,q}^{(k)}\}_{q=1}^{N_e}, \qquad k = 0, \ldots, N_\tau,$$

and the associated ensemble of reduced state solution

$$\mathcal{U}_n^{(k)} = \{\mathbf{u}_n(\boldsymbol{\mu}),\ \boldsymbol{\mu} \in \mathcal{P}_n^{(k)}\}, \qquad k = 0, \ldots, N_\tau.$$

Consequently, we also compute the means (11), the covariance (12) and the cross-covariances (13) by relying on the reduced-order quantities. Hence, starting from the initial ensemble $\{\mathcal{P}_n^{(0)}, \mathcal{U}_n^{(0)}\}$, directly sampled from the prior, the RB-EnKF can be built with a two-stage recursion, similarly to what done in Section Section 3:

1. *prediction stage*:
   - compute the reduced solution $\mathbf{u}_n^{(k+1)}$ of the forward ROM (17) on $[\tau^{(k)}, \tau^{(k+1)})$ with initial datum $\mathbf{u}_n^{(k)}(\boldsymbol{\mu}) \in \mathcal{U}_n^{(k)}$, and the output $\mathbf{s}_n^{(k+1)}$ for each $\boldsymbol{\mu} \in \mathcal{P}_n^{(k)}$;
   - compute the sample means $\overline{\mathbf{u}}_n^{(k+1)}$, $\overline{\mathbf{s}}_n^{(k+1)}$ and $\overline{\boldsymbol{\mu}}_n^{(k)}$;
   - compute the sample covariance $\mathbf{C}_{s_n s_n}^{(k+1)} \in \mathbb{R}^{s\times s}$ and the cross-covariance matrices $\mathbf{C}_{\mu_n s_n}^{(k)} \in \mathbb{R}^{d\times s}$ and $\mathbf{C}_{u_n s_n}^{(k+1)} \in \mathbb{R}^{n\times s}$, using formulas (12)–(14) by substituting $\mathbf{s}_h$, $\mathbf{u}_h$ and $\mathcal{P}_h^{(k-1)}$ with $\mathbf{s}_n$, $\mathbf{u}_n$ and $\mathcal{P}_n^{(k-1)}$, respectively;
2. *analysis stage*: update the state/parameter ensemble through the following *reduced KF updating formula*:

$$\begin{bmatrix} \boldsymbol{\mu}_{n,q}^{(k+1)} \\ \mathbf{u}_n^{(k+1)}(\boldsymbol{\mu}_{n,q}^{(k+1)}) \end{bmatrix} = \begin{bmatrix} \boldsymbol{\mu}_{n,q}^{(k)} \\ \mathbf{u}_n^{(k+1)}(\boldsymbol{\mu}_{n,q}^{(k)}) \end{bmatrix} + \begin{bmatrix} \mathbf{C}_{\mu_n s_n}^{(k+1)} \\ \mathbf{C}_{u_n s_n}^{(k+1)} \end{bmatrix} (\boldsymbol{\Gamma} + \mathbf{C}_{s_n s_n}^{(k+1)})^{-1}(\mathbf{s}_q^{(k+1)} - \mathbf{s}_n^{(k+1)}(\boldsymbol{\mu}_{n,q}^{(k)})), \tag{20}$$

   for each $q = 1, \ldots, N_e$.

In this way, we are neglecting the error between the ROM and the FOM, which nevertheless might affect the accuracy of the state/parameter estimation, as shown in the following section.

4.3 Effectivity of the RB-EnKF

We now want to prove that the state/parameter estimation given by the RB-EnKF converges, as long as the ROM dimension increases, to the one which would be obtained by relying on the full-order EnKF. To this aim, we compare the resulting state/parameter ensemble $\{\mathcal{P}^{(N_\tau)},\mathcal{U}^{(N_\tau)}\}$ with the reduced ones $\{\mathcal{P}_n^{(N_\tau)},\mathcal{U}_n^{(N_\tau)}\}$, for any dimension n. To this goal, let us denote by

$$\mathbf{e}^{(k)} = \begin{bmatrix} \mathbf{e}_\mu^{(k)} \\ \mathbf{e}_u^{(k)} \end{bmatrix} = \begin{bmatrix} \hat{\boldsymbol{\mu}}_h^{(k)} \\ \hat{\mathbf{u}}_h^{(k)} \end{bmatrix} - \begin{bmatrix} \hat{\boldsymbol{\mu}}_n^{(k)} \\ \mathbf{V}\hat{\mathbf{u}}_n^{(k)} \end{bmatrix}, \qquad k = 1, \dots, N_\tau - 1,$$

the error between the means $[\hat{\boldsymbol{\mu}}_n^{(k)}, \mathbf{V}\hat{\boldsymbol{u}}_n^{(k)}]^T$ and $[\hat{\boldsymbol{\mu}}_h^{(k)}, \hat{\boldsymbol{u}}_h^{(k)}]^T$ computed over the respective ensembles, at a given time $\tau^{(k)}$, $k = 1, \dots, N_\tau$. The following theorem provides a way to bound this error in terms of the error at the previous step and a combination of the discrepancies between the full-order and the reduced-order outputs $\|\bar{\mathbf{s}}_h^{(k)} - \bar{\mathbf{s}}_n^{(k+1)}\|$, cross-covariances $\|\mathbf{C}_{\mu_h s_h}^{(k)} - \mathbf{C}_{\mu_n s_n}^{(k)}\|$ (resp. $\|\mathbf{C}_{u_h s_h}^{(k)} - \mathbf{C}_{u_n s_n}^{(k)}\|$), and covariances $\|\mathbf{C}_{s_h s_h}^{(k)} - \mathbf{C}_{s_n s_n}^{(k)}\|$, weighted by computable factors depending on

$$\gamma_h^{(k)} = \|(\boldsymbol{\Gamma} + \mathbf{C}_{s_h s_h}^{(k)})^{-1}\| \qquad \gamma_n^{(k)} = \|(\boldsymbol{\Gamma} + \mathbf{C}_{s_n s_n}^{(k)})^{-1}\|,$$

where $\|\cdot\|$ denotes the Euclidean norm.

Theorem 2. *For any $0 < n < N_h$, $k = 1, \dots, N_\tau$, the following relationships hold:*

$$\|\mathbf{e}_\mu^{(k)}\| \leq \|\mathbf{e}_\mu^{(k-1)}\| + c_{\mu,1}^{(k)}\|\bar{\mathbf{s}}_h^{(k)} - \bar{\mathbf{s}}_n^{(k)}\| + c_{\mu,2}^{(k)}\|\mathbf{C}_{\mu_h s_h}^{(k)} - \mathbf{C}_{\mu_n s_n}^{(k)}\| + c_{\mu,3}^{(k)}\|\mathbf{C}_{s_h s_h}^{(k)} - \mathbf{C}_{s_n s_n}^{(k)}\|, \tag{21}$$

$$\|\mathbf{e}_u^{(k)}\| \leq \|\mathbf{e}_u^{(k-1)}\| + c_{u,1}^{(k)}\|\bar{\mathbf{s}}_h^{(k)} - \bar{\mathbf{s}}_n^{(k+1)}\| + c_{u,2}^{(k)}\|\mathbf{C}_{u_h s_h}^{(k)} - \mathbf{V}\mathbf{C}_{u_n s_n}^{(k)}\| + c_{u,3}^{(k)}\|\mathbf{C}_{s_h s_h}^{(k)} - \mathbf{C}_{s_n s_n}^{(k)})\|, \tag{22}$$

where

$$c_{\mu,1}^{(k)} = \gamma_h^{(k)}\|\mathbf{C}_{\mu_h s_h}^{(k)}\|, \qquad c_{u,1}^{(k)} = \gamma_h^{(k)}\|\mathbf{C}_{u_h s_h}^{(k)}\|,$$
$$c_{\mu,2}^{(k)} = c_{u,2}^{(k)} = \gamma_h^{(k)}\|\mathbf{s}^{(k)} - \bar{\mathbf{s}}_n^{(k)}\|,$$
$$c_{\mu,3}^{(k)} = \gamma_n^{(k)}\gamma_h^{(k)}\|\mathbf{C}_{\mu_n s_n}^{(k)}\|\|\mathbf{s}^{(k)} - \bar{\mathbf{s}}_n^{(k)}\|, \qquad c_{u,3}^{(k)} = \gamma_n^{(k)}\gamma_h^{(k)}\|\mathbf{V}\mathbf{C}_{u_n s_n}^{(k)}\|\|\mathbf{s}^{(k)} - \bar{\mathbf{s}}_n^{(k)}\|.$$

Proof. By averaging over the sample $\mathcal{P}^{(k-1)}$ of (15), we obtain the following update equation for the estimate $[\hat{\boldsymbol{\mu}}_h; \hat{\boldsymbol{u}}_h]$

$$\begin{bmatrix} \hat{\boldsymbol{\mu}}_h^{(k)} \\ \hat{\mathbf{u}}_h^{(k)} \end{bmatrix} = \begin{bmatrix} \hat{\boldsymbol{\mu}}_h^{(k-1)} \\ \hat{\mathbf{u}}_h^{(k-1)} \end{bmatrix} + \begin{bmatrix} \mathbf{C}_{\mu_h s_h}^{(k)} \\ \mathbf{C}_{u_h s_h}^{(k)} \end{bmatrix} (\boldsymbol{\Gamma} + \mathbf{C}_{s_h s_h}^{(k)})^{-1}(\mathbf{s}^{(k)} - \bar{\mathbf{s}}_h^{(k)}). \tag{23}$$

By doing the same on (20) we have

$$\begin{bmatrix} \hat{\boldsymbol{\mu}}_n^{(k)} \\ \hat{\mathbf{u}}_n^{(k)} \end{bmatrix} = \begin{bmatrix} \hat{\boldsymbol{\mu}}_n^{(k-1)} \\ \hat{\mathbf{u}}_n^{(k-1)} \end{bmatrix} + \begin{bmatrix} \mathbf{C}_{\mu_n s_n}^{(k)} \\ \mathbf{C}_{u_n s_n}^{(k)} \end{bmatrix} (\boldsymbol{\Gamma} + \mathbf{C}_{s_n s_n}^{(k)})^{-1}(\mathbf{s}^{(k)} - \bar{\mathbf{s}}_n^{(k)}). \tag{24}$$

By subtracting (24) from (23), we can express $\mathbf{e}^{(k)}$ as $\mathbf{e}^{(k)} = \mathbf{e}^{(k-1)} + \mathbf{e}_I^{(k)} + \mathbf{e}_{II}^{(k)}$, being

$$\mathbf{e}_I^{(k)} = \begin{bmatrix} \mathbf{C}_{\mu_h s_h}^{(k)} \\ \mathbf{C}_{u_h s_h}^{(k)} \end{bmatrix} (\boldsymbol{\Gamma} + \mathbf{C}_{s_h s_h}^{(k)})^{-1}(\bar{\mathbf{s}}_n^{(k)} - \bar{\mathbf{s}}_h^{(k)}),$$

$$\mathbf{e}_{II}^{(k)} = \left(\begin{bmatrix} \mathbf{C}_{\mu_h s_h}^{(k)} \\ \mathbf{C}_{u_h s_h}^{(k)} \end{bmatrix} (\boldsymbol{\Gamma} + \mathbf{C}_{s_h s_h}^{(k)})^{-1} - \begin{bmatrix} \mathbf{C}_{\mu_n s_n}^{(k)} \\ \mathbf{V}\mathbf{C}_{u_n s_n}^{(k)} \end{bmatrix} (\boldsymbol{\Gamma} + \mathbf{C}_{s_n s_n}^{(k)})^{-1} \right) (\mathbf{s}^{(k)} - \bar{\mathbf{s}}_n^{(k)}). \tag{25}$$

Then, the following error estimates hold

$$\|\mathbf{e}_{I,\mu}^{(k)}\| \leq c_{\mu,1}^{(k)}\|\bar{\mathbf{s}}_n^{(k)} - \bar{\mathbf{s}}_h^{(k)}\| \qquad \|\mathbf{e}_{I,u}^{(k)}\| \leq c_{u,1}^{(k)}\|\bar{\mathbf{s}}_n^{(k)} - \bar{\mathbf{s}}_h^{(k)}\|, \|, \tag{26}$$

where $c_{\mu,1}^{(k)} = \gamma_h^{(k)}\|\mathbf{C}_{\mu_h s_h}^{(k)}\|$ and $c_{u,1}^{(k)} = \gamma_h^{(k)}\|\mathbf{C}_{u_h s_h}^{(k)}$, respectively. On the other hand, by adding and subtracting in (25) the quantity

$$\begin{bmatrix} \mathbf{C}_{\mu_n s_n}^{(k)} \\ \mathbf{V}\mathbf{C}_{u_n s_n}^{(k)} \end{bmatrix} (\boldsymbol{\Gamma} + \mathbf{C}_{s_h s_h}^{(k)})^{-1}(\mathbf{s}^{(k)} - \bar{\mathbf{s}}_n^{(k)})$$

and rewriting the expression (25) as $\mathbf{e}_{II}^{(k)} = \mathbf{e}_{i}^{(k)} + \mathbf{e}_{ii}^{(k)}$, with

$$\mathbf{e}_{i}^{(k)} = \left(\begin{bmatrix} \mathbf{C}_{\mu_h s_h}^{(k)} \\ \mathbf{C}_{u_h s_h}^{(k)} \end{bmatrix} - \begin{bmatrix} \mathbf{C}_{\mu_n s_n}^{(k)} \\ \mathbf{V}\mathbf{C}_{u_n s_n}^{(k)} \end{bmatrix} \right) (\mathbf{\Gamma} + \mathbf{C}_{s_h s_h}^{(k)})^{-1} (\mathbf{s}^{(k)} - \overline{\mathbf{s}}_n^{(k)}),$$

$$\mathbf{e}_{ii}^{(k)} = \begin{bmatrix} \mathbf{C}_{\mu_n s_n}^{(k)} \\ \mathbf{V}\mathbf{C}_{u_n s_n}^{(k)} \end{bmatrix} \left((\mathbf{\Gamma} + \mathbf{C}_{s_n s_n}^{(k)})^{-1} - (\mathbf{\Gamma} + \mathbf{C}_{s_h s_h}^{(k)})^{-1} \right) (\mathbf{s}^{(k)} - \overline{\mathbf{s}}_n^{(k)}),$$

we have

$$\begin{aligned} \|\mathbf{e}_{i,\mu}^{(k)}\| &\leq c_{\mu,2}^{(k)} \|\mathbf{C}_{\mu_h s_h}^{(k)} - \mathbf{C}_{\mu_n s_n}^{(k)}\| \qquad c_{\mu,2}^{(k)} = \gamma_h^{(k)} \|(\mathbf{s}^{(k)} - \overline{\mathbf{s}}_n^{(k)})\|, \\ \|\mathbf{e}_{i,u}^{(k)}\| &\leq c_{u,2}^{(k)} \|\mathbf{C}_{u_h s_h}^{(k)} - \mathbf{V}\mathbf{C}_{u_n s_n}^{(k)}\| \qquad c_{u,2}^{(k)} = \gamma_h^{(k)} \|(\mathbf{s}^{(k)} - \overline{\mathbf{s}}_n^{(k)})\|. \end{aligned} \tag{27}$$

By applying the Sherman-Morrison-Woodbury Formula (see, e.g., Sect. 2.4 in [17]) we have that

$$(\mathbf{\Gamma} + \mathbf{C}_{s_n s_n}^{(k)})^{-1} - (\mathbf{\Gamma} + \mathbf{C}_{s_h s_h}^{(k)})^{-1} = (\mathbf{\Gamma} + \mathbf{C}_{s_n s_n}^{(k)})^{-1} (\mathbf{C}_{s_h s_h}^{(k)} - \mathbf{C}_{s_n s_n}^{(k)}) (\mathbf{\Gamma} + \mathbf{C}_{s_h s_h}^{(k)})^{-1},$$

and, consequently, $\|(\mathbf{\Gamma} + \mathbf{C}_{s_n s_n}^{(k)})^{-1} - (\mathbf{\Gamma} + \mathbf{C}_{s_h s_h}^{(k)})^{-1}\| \leq \gamma_n^{(k+1)} \gamma_h^{(k)} \|\mathbf{C}_{s_h s_h}^{(k)} - \mathbf{C}_{s_n s_n}^{(k)}\|$, whence the following bounds hold for $\mathbf{e}$

$$\|\mathbf{e}_{ii,\mu}^{(k)}\| \leq c_{\mu,3}^{(k)} \|\mathbf{C}_{s_h s_h}^{(k)} - \mathbf{C}_{s_n s_n}^{(k)}\|, \qquad \|\mathbf{e}_{II,u}^{(k)}\| \leq c_{u,3}^{(k)} \|\mathbf{C}_{s_h s_h}^{(k)} - \mathbf{C}_{s_n s_n}^{(k)}\|. \tag{28}$$

Finally, by combining (26), (27) and (28), we obtain (21)–(22). □

In order to obtain accurate estimates when employing our proposed RB-EnKF, we thus require the ROM to be able to generate similar means $\overline{\mathbf{s}}_n^{(k)}(\boldsymbol{\mu}) \approx \overline{\mathbf{s}}_h^{(k)}(\boldsymbol{\mu})$ and covariance matrices $\mathbf{C}_{s_n s_n}^{(k)} \approx \mathbf{C}_{s_h s_h}^{(k)}$ and $\mathbf{C}_{\mu_n s_n}^{(k)} \approx \mathbf{C}_{\mu_h s_h}^{(k)}$, for each $k = 1, \ldots, N_\tau$, to the ones which would have been provided by the FOM. From the previous proposition we can also prove an *asymptotic consistency* property, ensuring that the state/parameter estimated through the RB-EnKF converge to the ones estimated by the full-order EnKF, for $n, m_D \to N_h$.

Corollary 3. *Assume that for any RB dimension $n = 1, \ldots, N_h$ and DEIM dimension $m_D = 1, \ldots, N_h$, there exists $\epsilon^{(\ell)}(n, m_D) > 0$ such that*

$$\|\mathbf{u}_h^{(\ell)}(\boldsymbol{\mu}) - \mathbf{V}\mathbf{u}_n^{(\ell)}(\boldsymbol{\mu})\| \leq \epsilon^{(\ell)}(n, m_D), \qquad \forall \ell = 0, \ldots, N_t, \quad \forall \boldsymbol{\mu} \in \mathcal{P}$$

and that $\epsilon^{(\ell)}(n, m_D) \to 0$ for $n, m_D \to N_h$,. Then, it follows that

$$\|\hat{\boldsymbol{\mu}}_n - \hat{\boldsymbol{\mu}}_h\| \to 0, \qquad \|\mathbf{V}\hat{\mathbf{u}}_n - \hat{\mathbf{u}}_h\| \to 0 \qquad \text{for } n, m_D \to N_h.$$

Proof. Since the outputs $\mathbf{s}_h^{(k)}(\boldsymbol{\mu})$, $\mathbf{s}_n^{(k)}(\boldsymbol{\mu})$ are linear with respect to the solution $\mathbf{u}(t; \boldsymbol{\mu})$ of the dynamical system, it follows that, for any $\boldsymbol{\mu} \in \mathcal{P}$,

$$\|\mathbf{s}_h^{(k)}(\boldsymbol{\mu}) - \mathbf{s}_n^{(k)}(\boldsymbol{\mu})\| \leq \Delta t \|\mathbf{H}\| \sum_{K(k-1) \leq \ell \leq K(k)} \epsilon^{(\ell)}(n, m_D) \qquad \forall k = 1, \ldots, N_\tau. \tag{29}$$

Since the means and the covariance matrices of the quantities of interest are evaluated on different subsets $\mathcal{P}_h^{(k)}$ and $\mathcal{P}_n^{(k)}$ for each $k = 1, \ldots, N_\tau$, let us denote by

$$(\overline{\mathbf{s}}_n^{(k)})_{\mathcal{P}_h} = \frac{1}{N_e} \sum_{\boldsymbol{\mu} \in \mathcal{P}_h^{(k-1)}} \mathbf{s}_n^{(k)}(\boldsymbol{\mu}), \quad (\mathbf{C}_{s_n s_n}^{(k)})_{\mathcal{P}_h} = \frac{1}{N_e - 1} \sum_{\mu \in \mathcal{P}_h^{(k-1)}} (\mathbf{s}_n^{(k)}(\boldsymbol{\mu}) - (\overline{\mathbf{s}}_n^{(k)})_{\mathcal{P}_h})(\mathbf{s}_n^{(k)}(\boldsymbol{\mu}) - (\overline{\mathbf{s}}_n^{(k)})_{\mathcal{P}_h})^T,$$

the mean and the covariance of the reduced output over the full-order ensemble $\mathcal{P}_h$, respectively. Then, we can control the difference between the output means as

$$\|\overline{\mathbf{s}}_h^{(k)} - \overline{\mathbf{s}}_n^{(k)}\| \leq \|\overline{\mathbf{s}}_h^{(k)} - (\overline{\mathbf{s}}_n^{(k)})_{\mathcal{P}_h}\| + \|(\overline{\mathbf{s}}_n^{(k)})_{\mathcal{P}_h} - \overline{\mathbf{s}}_n^{(k)}\|$$

so that, by averaging (29) with respect to $\mathcal{P}_h$, we bound the first term as

$$\|\overline{\mathbf{s}}_h^{(k)} - (\overline{\mathbf{s}}_n^{(k)})_{\mathcal{P}_h}\| \leq \Delta t \|\mathbf{H}\| \sum_{K(k-1) \leq \ell \leq K(k)} \epsilon^{(\ell)}(n, m_D) \qquad \forall k = 1, \ldots, N_\tau.$$

Similarly, the difference between the covariance matrices can be bounded as

$$\|\mathbf{C}^{(k)}_{s_h s_h} - \mathbf{C}^{(k)}_{s_n s_n}\| \leq \|\mathbf{C}^{(k)}_{s_h s_h} - (\mathbf{C}^{(k)}_{s_n s_n})_{\mathcal{P}_h}\| + \|(\mathbf{C}^{(k)}_{s_n s_n})_{\mathcal{P}_h} - \mathbf{C}^{(k)}_{s_n s_n})\|$$

where the first term can be bounded as

$$\|\mathbf{C}^{(k)}_{s_h s_h} - (\mathbf{C}^{(k)}_{s_n s_n})_{\mathcal{P}_h}\| \leq c^{(k)}_{ss} \sum_{K(k-1)\leq \ell \leq K(k)} \epsilon^{(\ell)}(n, m_D) \qquad \forall k = 1, \dots, N_\tau,$$

with $c^{(k)}_{ss} = 4\Delta t \max_{\boldsymbol{\mu}\in\mathcal{P}^{(k-1)}} (\|\mathbf{s}^{(k)}_h(\boldsymbol{\mu}) - \overline{\mathbf{s}}^{(k)}_h\| + \|\mathbf{s}^{(k)}_n(\boldsymbol{\mu}) - \overline{\mathbf{s}}^{(k)}_n\|)$, being, for any couple of random vectors $\mathbf{x} = [\mathbf{x}_1, \mathbf{x}_2]^T, \mathbf{y} = [\mathbf{y}_1, \mathbf{y}_2]^T$,

$$\|C_{\mathbf{x}_1\mathbf{y}_1} - C_{\mathbf{x}_2\mathbf{y}_2}\| \leq (\|\mathbf{y}_1 - \overline{\mathbf{y}}_1\| + \|\mathbf{x}_2 - \overline{\mathbf{x}}_2\|)(\|\mathbf{x}_1 - \mathbf{x}_2\| + \|\overline{\mathbf{x}}_1 - \overline{\mathbf{x}}_2\| + \|\mathbf{y}_1 - \mathbf{y}_2\| + \|\overline{\mathbf{y}}_1 - \overline{\mathbf{y}}_2\|),$$

where $C_{\mathbf{xy}}$ denotes the cross-covariance matrix between $\mathbf{x}$ and $\mathbf{y}$; see e.g. [10].

Provided that $\mathcal{P}^{(0)}_h = \mathcal{P}^{(0)}_n$ and assuming that $\epsilon^{(\ell)}(n, m_D) \to 0$ for $n, m_D \to N_h$, we have that

$$\|\overline{\mathbf{s}}^{(k)}_h - (\overline{\mathbf{s}}^{(k)}_n)_{\mathcal{P}_h}\| \to 0, \qquad \|\mathbf{C}^{(k)}_{s_h s_h} - (\mathbf{C}^{(k)}_{s_n s_n})_{\mathcal{P}_h}\| \to 0, \qquad k = 1, \dots, N_\tau$$

and, consequently,

$$\|(\overline{\mathbf{s}}^{(k)}_n)_{\mathcal{P}_h} - \overline{\mathbf{s}}^{(k)}_n\| \to 0, \qquad \|(\mathbf{C}^{(k)}_{s_n s_n})_{\mathcal{P}_h} - \mathbf{C}^{(k)}_{s_n s_n})\| \to 0, \qquad k = 1, \dots, N_\tau.$$

In the same way, we can conclude that $\|\mathbf{C}^{(k+1)}_{u_h s_h} - \mathbf{C}^{(k+1)}_{u_n s_n})\|$ and $\|\mathbf{C}^{(k+1)}_{\mu_h s_h} - \mathbf{C}^{(k+1)}_{\mu_n s_n})\|$ are also controlled by $\epsilon^{(\ell)}(n, m_D)$, $\ell = Kk, \dots, K(k+1)$, thus yielding the fact that the right-hand sides of both (21) and (22) go to zero in the limit $n, m_D \to N_h$. □

5 Reduction error model

Using a ROM to evaluate the output of the forward PDE system greatly reduces the cost entailed by the solution of the entire Bayesian inverse problem without reducing the number of ensemble particles. Indeed, undersampling caused by small ensemble sizes would yield three remarkable problems in ensemble filtering: underestimation of covariance, filter divergence and the development of long-range spurious correlations. Sampling errors and their drawbacks can be mitigated by making use of inflation and localization of forecast covariances. The former consists in augmenting the variance of the additive noise model, whereas the latter properly modifies the prior ensemble to reduce filtering errors and avoid filter divergence (see e.g. [21, 18]).

The focus of this paper is rather on the mitigation of the reduction error, which can be seen as a form of *model error* or epistemic uncertainty affecting input/output evaluation. In the EnKF literature, this kind of problems arises when real observations are compared with simulated outputs [29, 18]. For the method at hand, the RB approximation automatically reduces the EnKF complexity, since the state vector dimension is reduced from N_h to $n \ll N_h$, thus enabling the use of sufficiently large ensembles. Nevertheless, to reduce the estimate bias introduced by the use of a ROM, we equip the RB-EnKF with a REM which aims at directly correcting the input/output evaluation. As detailed below, the REM also provides an additive inflation of the covariance matrix to ensure the accuracy of the results, although for the time being classical localization and inflation techniques are not adopted; their use, however, could enhance the accuracy of the estimates when even smaller ensemble size are considered for the sake of computational efficiency.

Indeed, by simply rewriting the additive error noise model (1), we get

$$\mathbf{s}^{(k)} = \mathbf{s}^{(k)}_n(\boldsymbol{\mu}^*) + \left(\mathbf{s}^{(k)}_h(\boldsymbol{\mu}^*) - \mathbf{s}^{(k)}_n(\boldsymbol{\mu}^*)\right) + \boldsymbol{\varepsilon}_{\text{noise}}, \qquad \forall k = 1, \dots, N_\tau; \tag{30}$$

hence, if the reduction error $\mathbf{s}^{(k)}_h(\boldsymbol{\mu}^*) - \mathbf{s}^{(k)}_n(\boldsymbol{\mu}^*)$ is not negligible with respect to $\boldsymbol{\varepsilon}_{\text{noise}}$, the RB-EnKF might yield biased estimates. Therefore, we introduce a statistical model for the reduction error $\boldsymbol{\varepsilon}^{(k)}_{\text{ROM}}(\boldsymbol{\mu})$, over each window $k = 1, \dots, N_\tau$, such that (30) can be replaced by

$$\mathbf{s}^{(k)} = \mathbf{s}^{(k)}_n(\boldsymbol{\mu}^*) + \hat{\boldsymbol{\varepsilon}}^{(k)}_{\text{ROM}}(\boldsymbol{\mu}^*) + \boldsymbol{\varepsilon}_{\text{noise}} \qquad \forall k = 1, \dots, N_\tau \tag{31}$$

and the evaluation of the deterministic quantity $\mathbf{s}^{(k)}_h(\boldsymbol{\mu}) - \mathbf{s}^{(k)}_n(\boldsymbol{\mu})$, which would however depend on the FOM solution, can thus be avoided.

To compute an estimate of $\boldsymbol{\varepsilon}_{\mathrm{ROM}}^{(k)}(\boldsymbol{\mu})$, which will be denoted hereon by $\hat{\boldsymbol{\varepsilon}}_{\mathrm{ROM}}^{(k)}(\boldsymbol{\mu})$ and to which we refer to as *reduction error model* (REM), we rely on the curve kriging method, a weighted interpolation technique for spatially-distributed functional data (see e.g. [16, 28]).

Let us denote by $S_{cal} = \{\boldsymbol{\mu}_1, \dots, \boldsymbol{\mu}_{N_{cal}}\}$ a *calibration set* made by N_{cal} parameter vectors, for which we need to determine N_{cal} queries to both the ROM and the FOM. We underline that these evaluations have to be performed only once, after the ROM has been built, and before the inversion procedure takes place. In particular, we can choose S_{cal} such that $S_{train} \subset S_{cal}$ so that we can take advantage of the snapshots already computed before running the POD, and ensure not to overestimate the reduction error in those training points.

We assume each component $\{\chi_t^{(j)}(\boldsymbol{\mu})\}$, $j = 1, \dots, s$, of the reduction error

$$\boldsymbol{\chi}_t(\boldsymbol{\mu}) = \mathbf{H}(\mathbf{u}_h(t;\boldsymbol{\mu}) - \mathbf{u}_n(t;\boldsymbol{\mu})) \in \mathbb{R}^s, \qquad t \in (0,T)$$

to be a functional random field, that is, a set of functional random variables indexed by $\boldsymbol{\mu} \in \mathcal{P}$, taking values in $L^2(a,b)$, with $(a,b) \subseteq (0,T)$. For each $j = 1, \dots, s$, the curve kriging method provides an estimate of the error over $(0,T)$, for any new $\boldsymbol{\mu}_0 \in \mathcal{P}$, as a linear combination of the reduction errors computed for the elements in the calibration set S_{cal}, that is,

$$\hat{\chi}_t^{(j)}(\boldsymbol{\mu}_0) = \sum_{q=1}^{N_{cal}} \lambda_q^{(j)}(\boldsymbol{\mu}_0)\chi_t^{(j)}(\boldsymbol{\mu}_q), \qquad \boldsymbol{\mu}_0 \in \mathcal{P}, \quad j = 1, \dots, s,$$

where the set of weights $\{\lambda_q^{(j)}(\boldsymbol{\mu}_0)\}_{q=1}^{N_{cal}}$ are computed by requiring that $\hat{\chi}_t^{(j)}$ is the best linear unbiased estimator of $\chi_t^{(j)}$, see Appendix A for a detailed construction.

Since we are interested to embed the REM into the KF updating formula for the sequential update of the ensemble on each window $[\tau^{(k)}, \tau^{(k+1)})$, we need to build a curve kriging predictor $\hat{\chi}_t^{(j)}(\boldsymbol{\mu})$ for each $j = 1, \dots, s$, on each window $[\tau^{(k-1)}, \tau^{(k)})$. As a matter of fact, our REM is given, for any $\boldsymbol{\mu} \in \mathcal{P}_c^{(k)}$ by integrating over $[\tau^{(k-1)}, \tau^{(k)})$ the kriging predictor, that is,

$$\hat{\boldsymbol{\varepsilon}}_{\mathrm{ROM}}^{(k)}(\boldsymbol{\mu}) \ : \hat{\varepsilon}_{ROM,j}^{(k)}(\boldsymbol{\mu}) = \int_{\tau^{(k-1)}}^{\tau^{(k)}} \hat{\chi}_t^{(j)}(\boldsymbol{\mu})dt. \tag{32}$$

The corresponding trace-variances (see equation (46) in Appendix A for the definition of γ_t and η)

$$\hat{\sigma}^2_{\hat{\chi}_t^{(j)}}(\boldsymbol{\mu}) = \sum_{q=1}^{N_{cal}} \lambda_q^{(j)}(\boldsymbol{\mu}) \int_{\tau^{(k-1)}}^{\tau^{(k)}} \gamma_t(\|\boldsymbol{\mu}_i - \boldsymbol{\mu}\|) - \eta$$

allows to define the (diagonal) covariance matrix

$$\hat{\boldsymbol{\Gamma}}_{\mathrm{ROM}}^{(k)}(\boldsymbol{\mu}) = \mathrm{diag}([\hat{\sigma}^2_{\hat{\chi}_t^{(1)}}(\boldsymbol{\mu}), \dots, \hat{\sigma}^2_{\hat{\chi}_t^{(s)}}(\boldsymbol{\mu})]). \tag{33}$$

This latter takes automatically into account the error committed by the REM in approximating the reduction error. The proposed REM thus yields an output correction $\hat{\varepsilon}_{\mathrm{ROM}}^{(k)}$ and an additional contribution $\hat{\boldsymbol{\Gamma}}_{\mathrm{ROM}}^{(k)}$ to the Kalman gain – which have indeed to be evaluated for each $k = 1, \dots, N_\tau$ and upon each ensemble particle – thus leading to the following *corrected (reduced) KF updating formula* to update the ensemble $\mathcal{P}_c^{(k)}$:

$$\begin{bmatrix} \boldsymbol{\mu}_{c,q}^{(k+1)} \\ \mathbf{u}_c^{(k+1)}(\boldsymbol{\mu}_{c,q}^{(k+1)}) \end{bmatrix} = \begin{bmatrix} \boldsymbol{\mu}_{c,q}^{(k)} \\ \mathbf{u}_c^{(k+1)}(\boldsymbol{\mu}_{c,q}^{(k)}) \end{bmatrix} + \begin{bmatrix} \mathbf{C}_{\mu_c s_c}^{(k+1)} \\ \mathbf{C}_{u_c s_c}^{(k+1)} \end{bmatrix} (\boldsymbol{\Gamma} + \hat{\boldsymbol{\Gamma}}_{\mathrm{ROM}}^{(k+1)}(\boldsymbol{\mu}_{c,q}^{(k)}) + \mathbf{C}_{s_c s_c}^{(k+1)})^{-1} (\mathbf{s}_q^{(k+1)} - \mathbf{s}_c^{(k+1)}(\boldsymbol{\mu}_{c,q}^{(k)})) \tag{34}$$

where $\mathbf{s}_c^{(k)}(\boldsymbol{\mu})$ represents the *corrected output*, i.e.

$$\mathbf{s}_c^{(k)}(\boldsymbol{\mu}) = \mathbf{s}_n^{(k)}(\boldsymbol{\mu}) + \hat{\boldsymbol{\varepsilon}}_{\mathrm{ROM}}^{(k)}(\boldsymbol{\mu}), \qquad \boldsymbol{\mu} \in \mathcal{P};$$

the sample covariance $\mathbf{C}_{s_c s_c}^{(k)}$ and cross-covariances $\mathbf{C}_{\mu_c s_c}^{(k)}$, $\mathbf{C}_{u_c s_c}^{(k)}$ are computed as in equations (12), (13) and (14) by substituting $\mathbf{s}_h$, $\mathbf{u}_h$ and $\mathcal{P}_h^{(k-1)}$ with $\mathbf{s}_c$, $\mathbf{u}_c$ and $\mathcal{P}_c^{(k-1)}$, respectively.

The use of our REM during the RB-EnKF thus only requires, at each iteration of the filtering procedure, to solve s linear systems (see equation (42)) of small dimension $(N_{cal}+1)\times(N_{cal}+1)$, to get the weights $\{\lambda_q^{(j)}\}_{q=1}^{N_{cal}}$ for each output component $j=1,\dots,s$. Each linear system requires to fit the so-called semi-variogram function γ_t on the calibration set, as described in Appendix A. A detailed description of the *corrected RB-EnKF* algorithm is finally reported in Algorithm 2.

Algorithm 2 Reduced basis Ensemble Kalman filter procedure

procedure RB-EnKF(+REM)
  Initialization
  $\{\mathcal{P}_c^{(0)},\mathcal{U}_c^{(0)}\} \leftarrow$ sampling N_e vectors from π_{prior}
  for $q=1:N_e$, $k=1:N_\tau$ **do**
    $\mathbf{s}_q^{(k)} \leftarrow \mathbf{s}_h^{(k)}(\boldsymbol{\mu}^*)+\boldsymbol{\varepsilon}_q^{(k)}$
  end for
    for $k=0:N_\tau-1$ **do**
      for j=1 : s **do**
        sample the empirical semi-variogram $\{(\delta_m,\hat{\gamma}(\delta_m))\}_{m=1}^M$, using (43)
        fit the parametric semi-variogram model (44) on the sample $\{(\delta_m,\hat{\gamma}(\delta_m))\}_{m=1}^M$
      end for
      Prediction stage:
      for $[\boldsymbol{\mu},\mathbf{u}_c^{(k)}(\boldsymbol{\mu})]^T \in \{\mathcal{P}_c^{(k)},\mathcal{U}_c^{(k)}\}$ **do**
        $\mathbf{u}_c^{(k+1)}(\boldsymbol{\mu}) \leftarrow$ solve forward problem (16) with initial datum $\mathbf{u}_n^{(k)}(\boldsymbol{\mu})$
        for j=1 : s **do**
          $\hat{\boldsymbol{\varepsilon}}_{\text{ROM}}^{(k+1)}(\boldsymbol{\mu}) \leftarrow$ solve linear system (42)
          $(\hat{\boldsymbol{\Gamma}}_{\text{ROM}}^{(k+1)})_{jj} \leftarrow$ evaluate (46)
        end for
        $\mathbf{s}_c^{(k+1)}(\boldsymbol{\mu}) = \mathbf{s}_n^{(k+1)}(\boldsymbol{\mu}) + \hat{\boldsymbol{\varepsilon}}_{\text{ROM}}^{(k+1)}(\boldsymbol{\mu})$
      end for
      compute means $\overline{\mathbf{s}}_c^{(k+1)}$, $\overline{\mathbf{u}}_c^{(k+1)}$, $\overline{\boldsymbol{\mu}}_c^{(k+1)}$
      compute (cross)-covariances $\mathbf{C}_{s_cs_c}^{(k+1)}$, $\mathbf{C}_{\mu_cs_c}^{(k+1)}$ and $\mathbf{C}_{u_cs_c}^{(k+1)}$
      Update stage:
      for $[\boldsymbol{\mu},\mathbf{u}_h^{(k+1)}(\boldsymbol{\mu})]^T \in \{\mathcal{P}_c^{(k)}\}$ **do**
        update each state/parameter particle using (34)
      end for
    end for
  end procedure

5.1 Effectivity of the proposed REM

We observe that the reduction error directly affects the quality of the likelihood function (10) from which we have derived the reduced KF updating formula. By defining the reduced likelihood as

$$\pi_n^{(k)} = \pi_n\left(\mathbf{s}^{(k+1)}\middle|\,[\boldsymbol{\mu},\mathbf{V}\mathbf{u}_n^{(k+1)}]^T\right) = (2\pi)^{(-\frac{s}{2})}|\boldsymbol{\Gamma}|^{-\frac{1}{2}}\exp\left\{-\frac{1}{2}\|\mathbf{s}^{(k+1)}-\mathbf{s}_n^{(k+1)}\|_{\boldsymbol{\Gamma}}\right\},$$

and the corrected likelihood as

$$\pi_c^{(k)} = (2\pi)^{(-\frac{s}{2})}|\boldsymbol{\Gamma}+\hat{\boldsymbol{\Gamma}}_{\text{ROM}}^{(k)}|^{-\frac{1}{2}}\exp\left\{-\frac{1}{2}\|\mathbf{s}^{(k+1)}-\mathbf{s}_c^{(k+1)}\|_{\boldsymbol{\Gamma}+\hat{\boldsymbol{\Gamma}}_{\text{ROM}}^{(k+1)}}\right\},$$

we can rely on the analysis provided in [27, Section 6] on the Kullback-Leibler (KL) divergence between the likelihood function $\pi^{(k)}$, $\pi_n^{(k)}$ and $\pi_c^{(k)}$ at each *prediction-analysis* step $k=1,\dots,N_\tau$. To this end, let us recall the notion of Kullback-Leibler (KL) divergence, which is a measure of the difference between two probability distributions π_A and π_B:

$$D_{KL}(\pi_A||\pi_B) = \int \pi_A(z)\log\left(\frac{\pi_A(z)}{\pi_B(z)}\right)dz.$$

In this case, we would obtain

$$D_{KL}(\pi^{(k)}||\pi_n^{(k)}) = \frac{1}{2}\sum_{j=1}^{s}\left(\frac{(\mathbf{s}_h^{(k+1)}(\boldsymbol{\mu}) - \mathbf{s}_n^{(k+1)}(\boldsymbol{\mu}))_j^2}{\boldsymbol{\Gamma}_{jj}}\right),$$

and

$$D_{KL}(\pi^{(k)}||\pi_c^{(k)}) = \frac{1}{2}\sum_{j=1}^{s}\left(\frac{(\mathbf{s}_h^{(k+1)}(\boldsymbol{\mu}) - \mathbf{s}_n^{(k+1)}(\boldsymbol{\mu}) - \hat{\boldsymbol{\varepsilon}}_{\mathrm{ROM}}^{(k+1)}(\boldsymbol{\mu}))_j^2}{\boldsymbol{\Gamma}_{jj} + (\hat{\boldsymbol{\Gamma}}_{\mathrm{ROM}}^{(k+1)})_{jj}(\boldsymbol{\mu})} + \frac{\boldsymbol{\Gamma}_{jj}}{\boldsymbol{\Gamma}_{jj} + (\hat{\boldsymbol{\Gamma}}_{\mathrm{ROM}}^{(k+1)})_{jj}(\boldsymbol{\mu})} - 1 - \log\left(\frac{\boldsymbol{\Gamma}_{jj}}{\boldsymbol{\Gamma}_{jj} + (\hat{\boldsymbol{\Gamma}}_{\mathrm{ROM}}^{(k+1)})_{jj}(\boldsymbol{\mu})}\right)\right).$$

To ensure that the KL divergence $D_{KL}(\pi||\pi_c)$ is smaller than $D_{KL}(\pi||\pi_n)$, we require that:

1. the REM correction is effective, that is

$$\mathbb{E}[\|\mathbf{s}_h^{(k)}(\boldsymbol{\mu}) - \mathbf{s}_c^{(k)}(\boldsymbol{\mu})\|] < \mathbb{E}[\|\mathbf{s}_h^{(k)}(\boldsymbol{\mu}) - \mathbf{s}_n^{(k)}(\boldsymbol{\mu})\|] \qquad \forall k = 1, \dots, N_\tau, \tag{35}$$

2. $(\hat{\boldsymbol{\Gamma}}_{\mathrm{ROM}}^{(k+1)})_{jj}$ is sufficiently small compared to $\boldsymbol{\Gamma}_{jj}$, $j = 1, \dots, s$.

Note that by construction $\mathbf{s}_h^{(k)}(\boldsymbol{\mu}) - \mathbf{s}_c^{(k)}(\boldsymbol{\mu}) = \mathbf{0}$ and $\hat{\boldsymbol{\Gamma}}_{\mathrm{ROM}}(\boldsymbol{\mu}) = \mathbf{0}$ for each $\boldsymbol{\mu} \in S_{cal}$. Since the noise is prescribed with a fixed covariance, the ROM and the REM construction can be suitably performed in order to ensure both the previous assumptions.

Remark 4. *Since the EnKF is based on a finite ensemble of particles, the distributions $\pi^{(k)}$, $\pi_n^{(k)}$ and $\pi_c^{(k)}$ are only approximated in the EnKF updating formula. It is sufficient to consider a large ensemble in order to avoid the propagation of additional sources of error.*

Note that the updating formula (34) could be derived using the corrected likelihood distribution $\pi_c^{(k)}$ instead of $\pi^{(k)}$. As a consequence, the ensemble updated through (34) provides a good approximation of the one obtained using (15) if the REM is effective. Moreover, under the two assumptions about the REM, the corrected ensemble $\mathcal{P}_c^{(k)}$ (and respectively $\mathcal{U}_c^{(k)}$) is considerably closer to $\mathcal{P}_h^{(k)}$ ($\mathcal{U}_h^{(k)}$) then $\mathcal{P}_n^{(k)}$ ($\mathcal{U}_n^{(k)}$). If we assume at each step $k = 1, \dots, N_\tau$ to use as initial datum the full-order ensemble $\mathcal{P}_h^{(k)}$ ($\mathcal{U}_h^{(k)}$), it is possible to prove that

$$\mathbb{E}[D_{KL}(\pi_{post}^{(k)}||\pi_{post,c}^{(k)})] < \mathbb{E}[D_{KL}(\pi_{post}^{(k)}||\pi_{post,n}^{(k)})]$$

where $\pi_{post}^{(k)}$, $\pi_{post,n}^{(k)}$ and $\pi_{post,c}^{(k)}$ denote respectively the full-order, the reduced-order and the corrected posterior distribution obtained by substituting the respective likelihood function $\pi^{(k)}$, $\pi_n^{(k)}$ and $\pi_c^{(k)}$ in (9); for further details see [27, Section 6.2].

As a matter of fact $\hat{\boldsymbol{\varepsilon}}_{\mathrm{ROM}}$ and $\hat{\boldsymbol{\Gamma}}_{\mathrm{ROM}}$ depend on either the number of basis functions and on the calibration set dimension. For this reason, in the numerical results we compare the errors $\|\hat{\boldsymbol{\mu}}_h - \hat{\boldsymbol{\mu}}_n\|$ and $\|\hat{\boldsymbol{\mu}}_h - \hat{\boldsymbol{\mu}}_c\|$ between the sample means and the errors between the relative covariance matrices $\|(\mathbf{C}_{\boldsymbol{\mu}_h,\boldsymbol{\mu}_h})^{1/2} - (\mathbf{C}_{\boldsymbol{\mu}_n,\boldsymbol{\mu}_n})^{1/2}\|$ and $\|(\mathbf{C}_{\boldsymbol{\mu}_h,\boldsymbol{\mu}_h})^{1/2} - (\mathbf{C}_{\boldsymbol{\mu}_c,\boldsymbol{\mu}_c})^{1/2}\|$ over the ensemble obtained with the full-order EnKF ($\mathcal{P}_h$), the RB-EnKF ($\mathcal{P}_n$) and the corrected RB-EnKF ($\mathcal{P}_c$) varying the number of basis functions and the calibration set dimension.

6 Numerical results

We present some numerical results obtained with the proposed RB-EnKF procedure for the estimation of unknown parameters/fields in a FitzHugh-Nagumo and a Fisher-Kolmogorov model*; the dynamics described by those two nonstationary nonlinear diffusion-reaction PDEs involve traveling front. Our aim is to study the impact of the reduction error on the state/parameter estimation and of the proposed REM on improving the accuracy of the results.

*Computations have been run on a laptop with a 2,2 GHz Intel Core i7 processor and 8 GB of RAM.

6.1 Test case 1

We consider the FitzHugh-Nagumo equations [13], which model the activation/deactivation dynamics of an excitable system, e.g., a neuron or a cardiac cell. In particular, we consider the test case proposed in [4]: given the parameter vector $\boldsymbol{\mu} = [\mu_1, \mu_2, \mu_3]^T$, $\forall t \in (0, T)$, find the couple $[u(t; \boldsymbol{\mu}), w(t; \boldsymbol{\mu})]$, $x \in \Omega = (0, 1)$, such that:

$$\begin{cases} \nu u_t(t;\boldsymbol{\mu}) = \nu^2 u_{xx}(t;\boldsymbol{\mu}) + \mathcal{N}(u(t;\boldsymbol{\mu})) - w(t;\boldsymbol{\mu}) + \mu_2 & x \in \Omega,\ t \in (0,T) \\ w_t(t;\boldsymbol{\mu}) = \mu_1 u(x,t) - \gamma u(x,t) + \mu_2 & x \in \Omega,\ t \in (0,T) \\ u_x(t;\boldsymbol{\mu}) = -50000 t^3 e^{-15t} & x = 0,\ t \in (0,T) \\ u_x(t;\boldsymbol{\mu}) = 0 & x = 1,\ t \in (0,T) \\ u(0;\boldsymbol{\mu}) = 0, \qquad w(0,\boldsymbol{\mu}) = 0 & x \in \Omega; \end{cases} \tag{36}$$

we define a cubic nonlinear term $\mathcal{N}(u) = u(u - 0.1)(1 - u)$, and set $\gamma = 2$,

$$\epsilon = 0.015(1 - \mu_3) \exp\left(-\frac{(x - 0.6)^2}{0.04}\right).$$

The semi-discretized FE approximation of problem (36) based on a partition of Ω into 1024 elements and linear finite elements yields an ODE system which can be written under the form (2). By considering a time discretization based on $N_t = 800$ time-steps and the implicit Euler method, we obtain a dynamical system under the form (3). Then, we consider as output

$$\mathbf{s}_h^{(k+1)} = \begin{bmatrix} \int_{\tau^{(k)}}^{\tau^{(k+1)}} \mathbf{u}_h(t;\boldsymbol{\mu})|_{x=0} dt \\ \int_{\tau^{(k)}}^{\tau^{(k+1)}} \mathbf{u}_h(t;\boldsymbol{\mu})|_{x=1} dt \end{bmatrix} \in \mathbb{R}^2 \qquad \forall k = 0, \dots, N_\tau - 1.$$

The goal of the inverse problem is to estimate $\boldsymbol{\mu}^*$ from a noisy output measurement $\mathbf{s} = \mathbf{s}_h(\boldsymbol{\mu}^*) + \boldsymbol{\varepsilon}_{\text{noise}}$, with $\boldsymbol{\varepsilon}_{\text{noise}} \sim \mathcal{N}(0, \sigma^2 I)$ exploiting the RB-EnKF procedure detailed in the paper and comparing the results obtained with the full-order EnKF. We take a Gaussian prior, so that $\boldsymbol{\mu} \in \mathcal{N}(\boldsymbol{\mu}_{\text{prior}}, \Sigma_{\text{prior}})$, with:

$$\boldsymbol{\mu}_{\text{prior}} = [0.7, 0.07, 0.76]^T, \qquad \Sigma_{\text{prior}} = \text{diag}([4 \cdot 10^{-4}, 9 \cdot 10^{-5}, 4 \cdot 10^{-3}]^T).$$

The discretized solution $[\mathbf{u}_h, \mathbf{w}_h]^T$ of the forward problem for the choice

$$\boldsymbol{\mu}^* = [0.6331, 0.0985, 0.7197]^T$$

is represented in Fig. 2. This is hereon considered as the *true* parameter vector value, which generate the data $\mathbf{s}$. We first solve the state/parameter estimation with the *full-order* EnKF

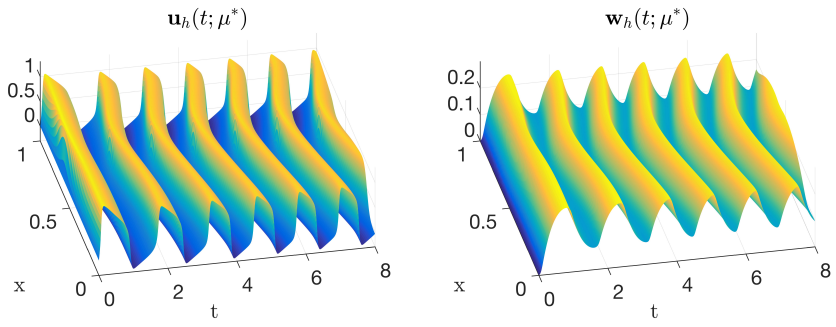

Figure 2: FE approximation of the forward problem for $\boldsymbol{\mu} = \boldsymbol{\mu}^*$.

starting from data measurements with different noise levels, in particular by considering $\sigma = 5\sigma_0$ and $\sigma = \sigma_0$, with $\sigma_0 = 0.033$. By looking at the behavior of the estimate $\hat{\boldsymbol{\mu}}_h$ in Fig. 3 for each component of the parameter vector, we observe that a faster convergence of the estimate to the *true* parameter value during the inversion procedure is achieved in the case of a smaller standard deviation (σ_0 with respect to $5\sigma_0$) on the noise.

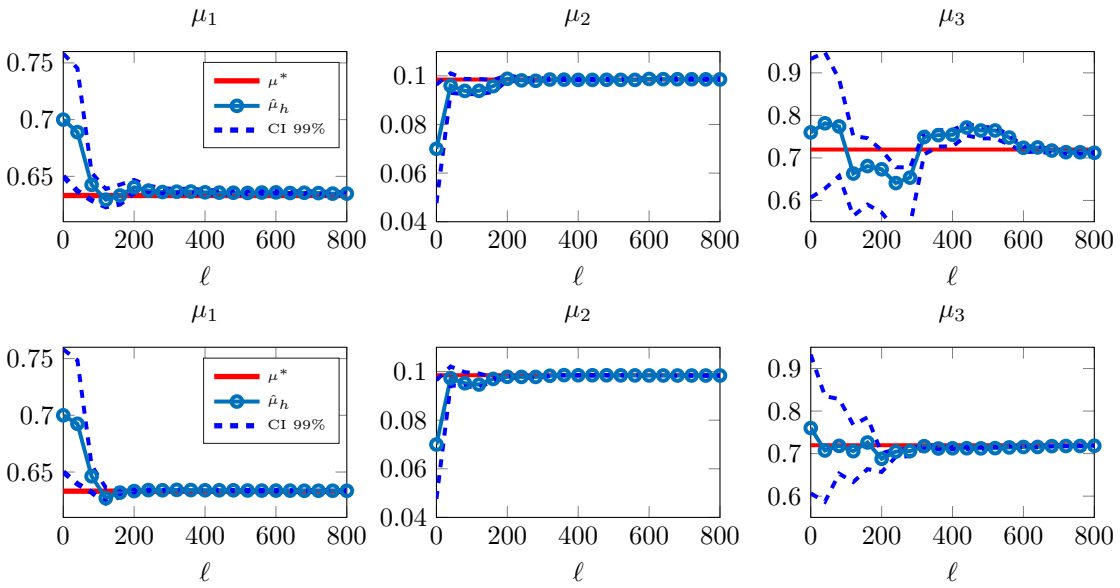

Figure 3: Comparison between $\boldsymbol{\mu}^*$ and $\{\hat{\boldsymbol{\mu}}_h^{(k)}\}_{k=1}^{N_\tau}$ for $\sigma = 5\sigma_0$ (first row) $\sigma = \sigma_0$ (second row), using $N_e = 500$ particles. The lower the noise level, the faster the convergence to $\boldsymbol{\mu}^*$ during the state/parameter estimation procedure (see e.g. the figures on the third column, related to the component μ^3).

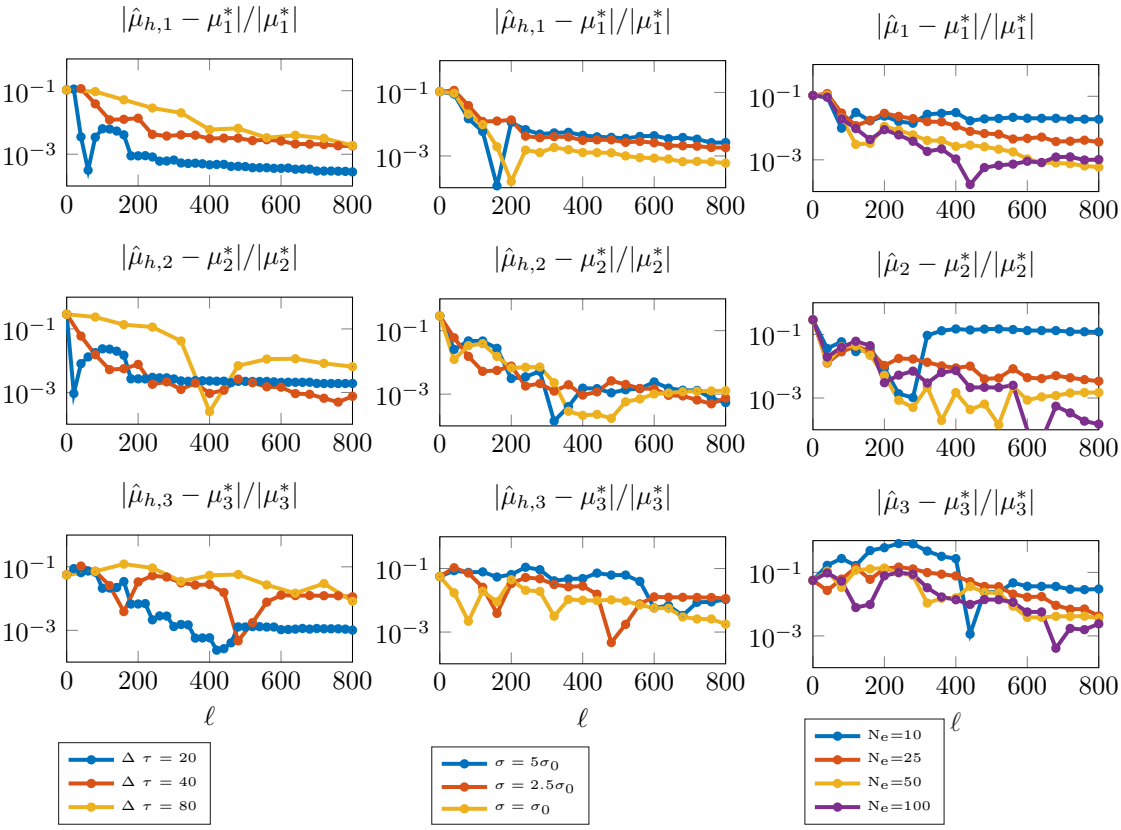

Figure 4: Relative error on estimated parameter components $|\mu^* - \hat{\mu}_h^{(k)}|/|\mu^*|$ with respect to the updating time-discretization (left), noise standard deviation (center) and ensemble size (right).

Next, we compare the solution of the state/parameter estimation problem obtained by varying the window length $\Delta\tau$, the noise standard deviation and the ensemble size N_e (see Fig. 4) taking $m_D = 15$ DEIM elements and $n = [7, 11, 15]$ basis function on the RB approximation. As expected, the estimates improve if both the noise $\boldsymbol{\varepsilon}_{\text{noise}}$ and $\Delta\tau$ decrease. While the former is a datum of the problem, the latter can be properly tuned (and reduced) to improve the estimation of the quantities of interest by slightly increasing the whole computational costs. In Fig. 5 we also study the state estimation with respect to the number of ROM basis functions: the reduction error clearly affects the estimation of this quantity.

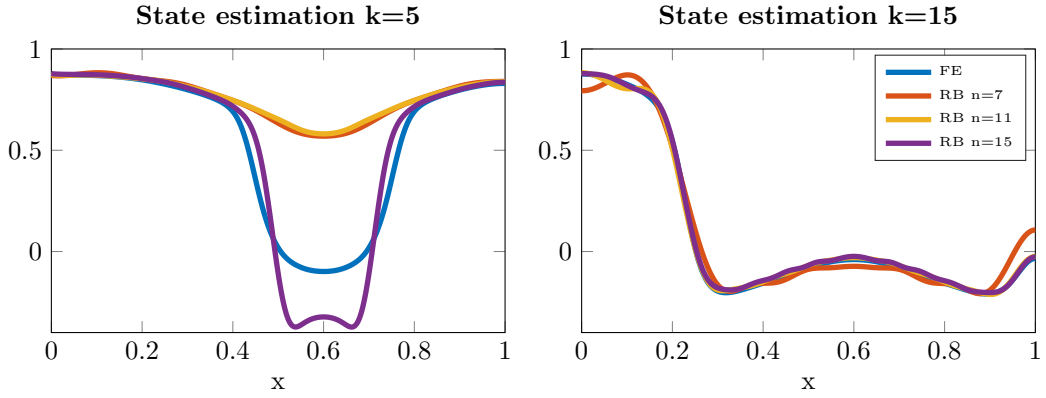

Figure 5: State estimation versus RB dimension n, at two different iterations ($k = 5$, left; $k = 15$, right) of the RB-EnKF.

Then, we consider the solution of the estimation problem by exploiting the RB-EnKF not including the REM correction. By looking at Fig. 6, we note that the estimate $\hat{\boldsymbol{\mu}}_n$ is not as accurate as the FOM estimate $\hat{\boldsymbol{\mu}}_h$, except for the case $n = 15$ and $\sigma = 5\sigma_0$, because of the propagation of the reduction error on the solution (see Fig. 6) and, consequently, on the measured outputs $\mathbf{s}_n$. These numerical results empirically confirm the theoretical findings of Proposition Theorem 2 and Corollary Theorem 3 in Section 4.3.

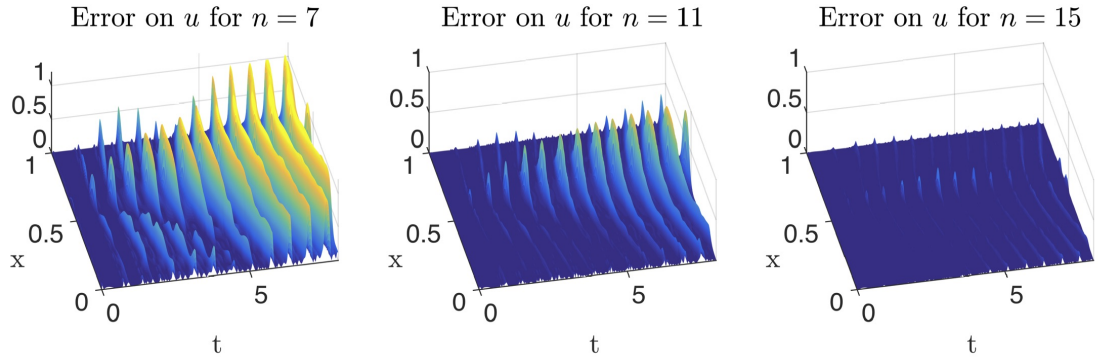

Figure 6: Error $|\mathbf{u}_h(t;\boldsymbol{\mu}^*) - \mathbf{u}_n(t;\boldsymbol{\mu}^*)|$ between the FOM and the ROM for different choices of the RB dimension $n = 7, 11, 15$ (from left to right).

Using a REM is therefore essential for improving the accuracy of the estimates of the RB-EnKF: as a matter of fact, the proposed REM based on curve kriging improves the parameter estimation in our RB-EnKF up to two orders of magnitude in some cases, as shown in Fig. 7.

More detailed results can be found in Table 1: for a noise level $\sigma = \sigma_0$, the ROM affects the accuracy of the estimation for every choice of n, while for higher noise levels the estimation error can be much smaller at least for larger RB dimensions (see e.g. the results obtained for $n = 15$). This because the reduction error for $n = 15$ is considerably small.

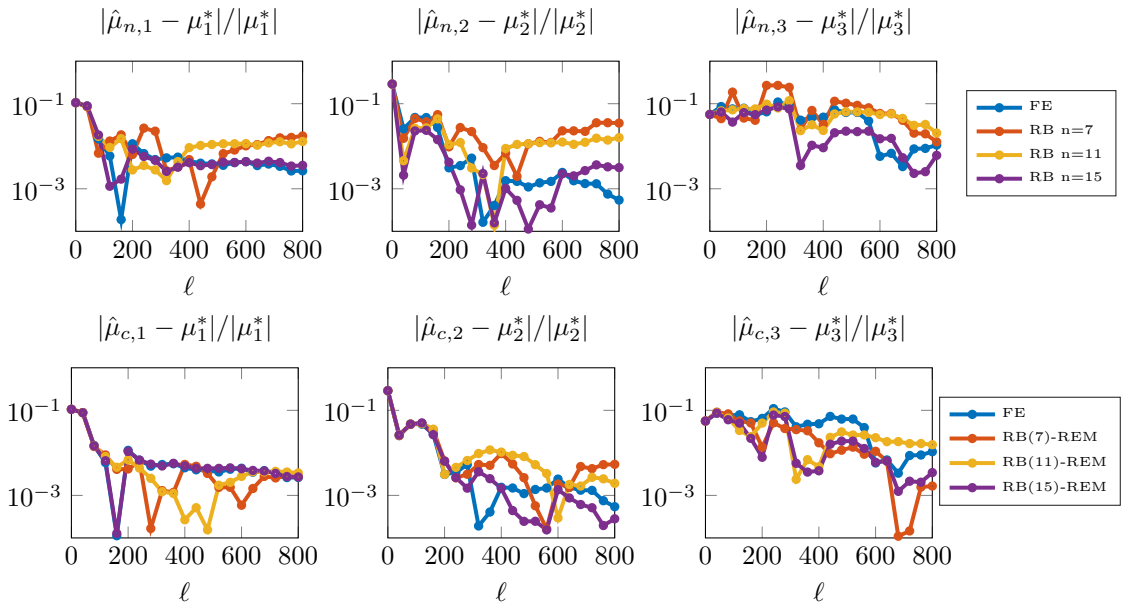

Figure 7: Relative error on estimated parameter components $|\mu^* - \hat{\mu}_n^{(k)}|/|\mu^*|$ versus the RB dimension n for the RB-EnKF (left) and its REM corrected version with $|S_{train}| = 80$ (right). By relying on the proposed REM, we obtain a relevant improvement of the estimates. Here the noise variance is $\sigma = 5\sigma_0$.

	σ	$n = 7$	$n = 11$	$n = 15$
	$5\sigma_0$	$0.0442\ (1.49 \cdot 10^{-4})$	$0.0365\ (2.01 \cdot 10^{-4})$	$0.0054\ (3.11 \cdot 10^{-5})$
RB-Enkf	$2.5\sigma_0$	$0.1594\ (6.11 \cdot 10^{-5})$	$0.0488\ (2.37 \cdot 10^{-4})$	$0.0070\ (3.47 \cdot 10^{-5})$
	σ_0	$0.1779\ (4.09 \cdot 10^{-5})$	$0.0708\ (2.59 \cdot 10^{-5})$	$0.0613(2.04 \cdot 10^{-5})$
	$5\sigma_0$	$0.0148\ (3.37 \cdot 10^{-4})$	$0.0265\ (1.01 \cdot 10^{-3})$	$0.0073\ (2.25 \cdot 10^{-4})$
RB-Enkf(+REM)	$2.5\sigma_0$	$0.0175\ (1.24 \cdot 10^{-4})$	$0.0226\ (9.63 \cdot 10^{-4})$	$0.0117\ (2.84 \cdot 10^{-4})$
	σ_0	$0.0058\ (1.95 \cdot 10^{-4})$	$0.0108\ (5.85 \cdot 10^{-4})$	$0.0059\ (2.82 \cdot 10^{-4})$

Table 1: Errors $\|\hat{\boldsymbol{\mu}}_h - \hat{\boldsymbol{\mu}}_n\|$ ($\|(\mathbf{C}^{(N_\tau)}_{\boldsymbol{\mu}_h,\boldsymbol{\mu}_h})^{1/2} - (\mathbf{C}^{(N_\tau)}_{\boldsymbol{\mu}_n,\boldsymbol{\mu}_n})^{1/2}\|$) and $\|\hat{\boldsymbol{\mu}}_h - \hat{\boldsymbol{\mu}}_c\|$ ($\|(\mathbf{C}^{(N_\tau)}_{\boldsymbol{\mu}_h,\boldsymbol{\mu}_h})^{1/2} - (\mathbf{C}^{(N_\tau)}_{\boldsymbol{\mu}_c,\boldsymbol{\mu}_c})^{1/2}\|$) versus the RB space dimension n and the noise variance σ. Our REM considerably improves the accuracy of the estimates: the error on the estimated parameter vector $\|\hat{\boldsymbol{\mu}}_h - \hat{\boldsymbol{\mu}}_n\|$ decreases by an order of magnitude for $n = 7$ whereas the error on the covariance matrices $\|(\mathbf{C}^{(N_\tau)}_{\boldsymbol{\mu}_h,\boldsymbol{\mu}_h})^{1/2} - (\mathbf{C}^{(N_\tau)}_{\boldsymbol{\mu}_n,\boldsymbol{\mu}_n})^{1/2}\|$ is still negligible with respect to the error $\|\hat{\boldsymbol{\mu}}_h - \hat{\boldsymbol{\mu}}_n\|$.

We recall that the REM is constructed only once after the ROM has been built. Given the reduction error $\boldsymbol{\chi}_t(\boldsymbol{\mu})$ for each $\boldsymbol{\mu} \in S_{cal}$, we check the assumptions of the functional kriging interpolation (see Appendix A). As shown in Fig. 8 for the case $N_{train} = 80$ and $n = 11$, the correlation between errors shows a dependence on the parameter location: parameters with small lag present a smaller variability with respect to parameters with a larger lag. Then, we estimated the empirical semi-variogram $\{\hat{\gamma}(\delta_1), \ldots, \hat{\gamma}(\delta_8)\}$ using (43) at 8 discrete lags $\{\delta_1, \ldots, \delta_8\}$ for each component of the output and on each window $(\tau^{(k)}, \tau^{(k+1)})$. Through these estimated values the spherical semi-variogram model (44) is fitted and then used to compute the corresponding matrix of the linear system (42). An example of empirical semi-variograms and relative semi-variograms model is presented in Fig. 8.

The use of REM allows to improve the accuracy of $\hat{\boldsymbol{\mu}}_c$ in any case, when the RB dimension n. In Fig. 7 we show the results obtained constructing a REM with $N_{train} = 80$ and $N_{cal} = 240$ samples. The quality of the REM yields significant improvements not only on the estimated means $\hat{\boldsymbol{\mu}}_c$, but also on the covariance matrix of the parameter ensemble $\mathbf{C}^{(N_\tau)}_{\mu\mu}$. If we compare the errors $\|\hat{\boldsymbol{\mu}}_h - \hat{\boldsymbol{\mu}}_n\|$ and $\|\hat{\boldsymbol{\mu}}_h - \hat{\boldsymbol{\mu}}_c\|$ between the estimates obtained with the full-order KF ($\hat{\boldsymbol{\mu}}_h$), the RB-

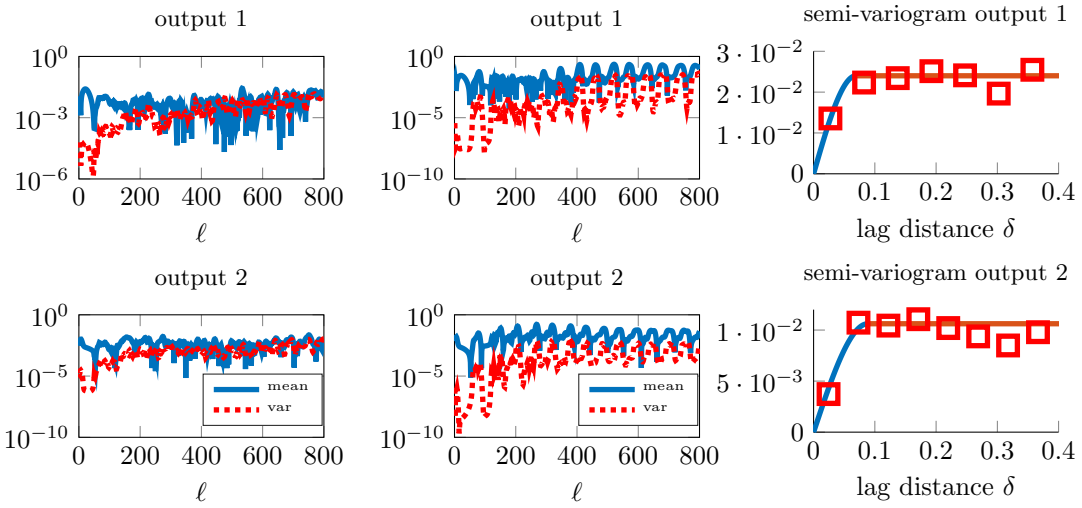

Figure 8: Sample means and covariances of the errors on both output components evaluated over samples $N(\delta_1)$ (left), $N(\delta_2)$ (right), $\delta_1 \ll \delta_2$. Estimated semi-variogram $\{\hat{\gamma}(\delta_1), \dots, \hat{\gamma}(\delta_8)\}$ (red squares) and fitted spherical model γ for the two output components on the time interval $(a, b) = (0, T)$

EnKF ($\hat{\boldsymbol{\mu}}_n$) and the corrected RB-EnKF ($\hat{\boldsymbol{\mu}}_c$), we find that $\|\hat{\boldsymbol{\mu}}_h - \hat{\boldsymbol{\mu}}_c\|$ is smaller than $\|\hat{\boldsymbol{\mu}}_h - \hat{\boldsymbol{\mu}}_n\|$ in all the considered cases, differing in some cases by more than two orders of magnitude. Also the error $\|(\mathbf{C}^{(N_\tau)}_{\boldsymbol{\mu}_h,\boldsymbol{\mu}_h})^{1/2} - (\mathbf{C}^{(N_\tau)}_{\boldsymbol{\mu}_c,\boldsymbol{\mu}_c})^{1/2}\|$ between the square roots of covariance matrices is considerably smaller than the error on the mean $\|\hat{\boldsymbol{\mu}}_h^{(N_\tau)} - \hat{\boldsymbol{\mu}}_c^{(N_\tau)}\|$, as we can observe in Table 1. This means that the correction introduced by the REM is able to correct the bias yielded by the propagation of the reduction error, without modifying substantially the distribution of the ensemble particles. The ensemble $\mathcal{P}_c^{(N_\tau)}$ resulting from the application of the corrected RB-EnKF is therefore closer to $\mathcal{P}_h^{(N_\tau)}$, the ensemble given by the full-order EnKF, than $\mathcal{P}_n^{(N_\tau)}$, the ensemble given by the RB-EnKF, as we have proven in Section 5.1.

		$N_{cal} = 0$	$N_{cal} = 24$	$N_{cal} = 80$	$N_{cal} = 240$
$N_{train} = 24$	$n = 7$	0.6669	0.1490	0.0250	0.0361
	$n = 11$	0.0465	0.0337	0.0152	0.0140
	$n = 15$	0.0385	0.0118	0.0161	0.0082
$N_{train} = 80$	$n = 7$	0.1594	–	0.0218	0.0175
	$n = 11$	0.0488	–	0.0398	0.0226
	$n = 15$	0.0070	–	0.0075	0.0117

Table 2: Relative error $\|\boldsymbol{\mu}^* - \hat{\boldsymbol{\mu}}_c\|/\|\hat{\boldsymbol{\mu}}\|$ versus the dimension $N_{train} = |S_{train}|$ of the training set and $N_{cal} = |S_{cal}|$ of the calibration set. The error decreases as soon as the S_{train} and S_{cal} have a large dimension. The case with $N_{cal} < N_{train}$ is meaningless, since we would ignore part of the already computed data within the training set.

As we can observe in Table 3, building a RB approximation of small dimension n over a training set with dimension $N_{cal} = 24$ (resp. $N_{cal} = 80$) requires an *offline* CPU time of 16 *min* (resp 53 *min*), which is small compare to the 387 *min* requested by the full-order EnKF procedure. In this setting, the calibration of the REM over sets of comparable dimension ($N_{cal} = 24$ and $N_{cal} = 80$) can be performed in few seconds. On the other hand, considering a calibration sample of large dimension $N_{cal} = 240$ yields more accurate results, however entailing a remarkable increase of the calibration costs. The solution of the state/parameter estimation problem using the corrected RB-EnKF entails only 11 *min*: by comparing the whole procedures, in the worst case scenario we are saving 219 *min*, i.e. more than the 55% of the total computational cost. We also pointed out that the computational saving is even larger if more than one state/parameter estimation problem

has to be solved, for instance on varying the noisy data $\mathbf{s}$: in this case the basis computation and the calibration need not to be run again, the only additional costs being those involved by the filtering procedure.

	RB			FE
	$n = 7$	$n = 11$	$n = 15$	$N_h = 1024$
dof reduction	99.3%	98.9%	98.5%	0%
Forward solution	0.6 s	0.7 s	0.8 s	40 s
$\lvert S_{train}\rvert = 24$				
ROM construction	16 min	16 min	16 min	
REM cal. $N_{cal} = 24$	15.1 s	17.4 s	18.73 s	
REM cal. $N_{cal} = 80$	37 min	37.1 min	37.3 min	
REM cal. $N_{cal} = 240$		139.2 min	139.3 min	139.4 min
$\lvert S_{train}\rvert = 80$				
ROM construction	53 min	53 min	53 min	
REM cal. $N_{cal} = 24$	15.1 s	17.4 s	18.73 s	
REM cal. $N_{cal} = 80$	49.8 s	53.8 s	59.7 s	
REM cal. $N_{cal} = 240$		103.3 min	103.4 min	103.5 min
State/parameter estimation problem				
EnKF time	6 min	6.3 min	6.9 min	387 min
EnKF REM $N_{cal} = 24$	7.7 min	8.2 min	8.6 min	
EnKF REM $N_{cal} = 80$	8.9 min	9 min	9.4 min	
EnKF REM $N_{cal} = 240$	10.9 min	11.1 min	11.4 min	

Table 3: Test case 1: computational performances of the estimation procedure (offline construction and online inversion stages) and comparison with the FOM case.

6.2 Test case 2

As second test case, we consider the Fisher-Kolmogorov-Petrovski-Piskunov reaction-diffusion equation, which models the dynamics of patterns in reactive media e.g. arising in combustion, spreading of epidemics and transport of chemicals in cells (see, e.g. [36]). Here we consider a two dimensional domain $\Omega \subset \mathbb{R}^2$ and formulate the forward problem as: find $u = u(t; \boldsymbol{\mu})$ s.t.

$$\begin{cases} \dfrac{\partial u}{\partial t} - \operatorname{div}(\nu(\mathbf{x}; \boldsymbol{\mu})\nabla u) + \mathcal{N}(u) = 0 & \mathbf{x} \in \Omega, t \in (0, T) \\ \nu(\mathbf{x}; \boldsymbol{\mu})\nabla u(t; \boldsymbol{\mu}) \cdot \mathbf{n} = 0 & \mathbf{x} \in \partial\Omega,\ t \in (0, T) \\ u(0; \boldsymbol{\mu}) = e^{-((x_1 - 1.5)^2 + 50x_2^2))} & \mathbf{x} \in \Omega, \end{cases} \tag{37}$$

where $\mathcal{N}(u) = 75u(1 - u)$ and the spatial domain Ω is given

$$\Omega = \left\{ (\rho, \vartheta) \in (1, 1.5) \times (0, \pi/2) :\ \rho = \sqrt{x_1^2 + x_2^2},\ \ \vartheta = \arctan\left(x_2/x_1\right) \right\}.$$

This particular shape of Ω imposes a preferential propagation of the front modeled by (37) along the tangential component of the arc. The semi-discretized FE approximation of problem (37) based on a partition of Ω using $N_h = 2768$ mesh nodes and linear finite elements yields a system of ODEs like the one in (2). By considering a partition of the time interval $(0, T)$ into $N_t = 140$ time-steps ($\Delta t = 1.1 \cdot 10^{-3}$) and the implicit Euler method, we obtain the dynamical system (3). Then, we consider eight outputs of the form:

$$s_j(t) = \int_\Omega \frac{1}{0.05\pi}\ \exp\left(-\frac{(x_1 - x_{cj})^2 + (x_2 - y_{cj})^2}{2(0.025)^2} \right) u(t; \boldsymbol{\mu}) d\Omega, \qquad j = 1, \ldots, 8,$$

where $(x_{cj}, y_{cj}) = (\rho\cos\theta, \rho\sin\theta)$ are given by all the possible combinations $\rho = \{1, 1.5\}$ and $\theta = \{\pi/6, \pi/4, \pi/3, \pi/2\}$. They represent approximated pointwise measurements of the quantities of interest $u(t; \boldsymbol{\mu})$. To show the reliability of our procedure in the solution of large-scale

state/parameter estimation problems, we consider a parametric field description of the diffusion coefficient ν of the form

$$\nu(\mathbf{x}, \boldsymbol{\mu}) = \mathbf{1} + \sum_{i=1}^{d} \mu_i \sqrt{\lambda_i} \boldsymbol{\xi}_i \tag{38}$$

where μ_i, $1 \leq i \leq d$ play the role of identifiable parameters, and $\boldsymbol{\xi}_1, \boldsymbol{\xi}_2, \ldots, \boldsymbol{\xi}_d$ are the d most relevant eigenmodes corresponding to the largest eigenvalues of the covariance matrix C

$$C_{ij} = a \exp\left(-\frac{\|\mathbf{x}^{(i)} - \mathbf{x}^{(j)}\|}{2b^2}\right) + c\delta_{ij} \qquad \forall i, j = 1, \ldots, N_h,$$

where $a, b, c > 0$ and $\{\mathbf{x}^{(i)}\}_{i=1}^{N_h}$ are the nodes of the computational mesh. The parametric field (38) is the Karhunen-Loève expansion (up to term d) of the Gaussian random field $\nu \sim \mathcal{N}(\mathbf{0}, C)$, where the prescribed covariance matrix C describes the spatial smoothness of the random field ν.

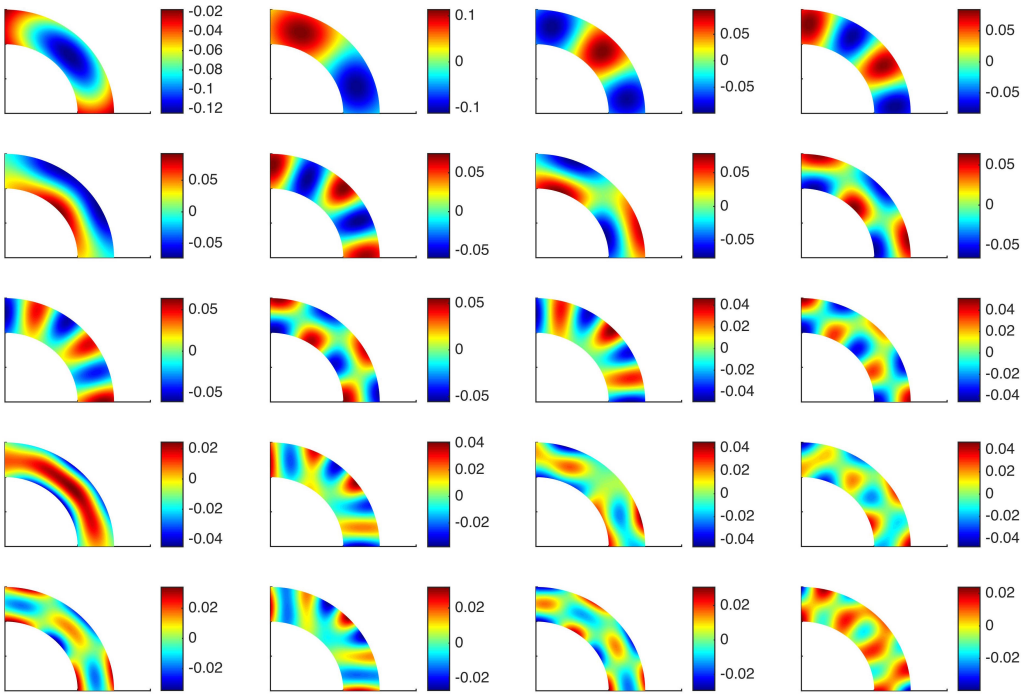

Figure 9: First $d = 20$ most relevant field modes of the Karhunen-Loève expansion of $\nu(\mathbf{x}, \boldsymbol{\mu})$.

The goal of the state/parameter estimation problem is to estimate $\boldsymbol{\mu}^*$ from noisy data with $\boldsymbol{\varepsilon}_{\text{noise}} \sim \mathcal{N}(0, \sigma^2 I)$. The prior distribution of $\boldsymbol{\mu}$ is Gaussian, $\boldsymbol{\mu} \in \mathcal{N}(\boldsymbol{\mu}_{\text{prior}}, \Sigma_{\text{prior}})$, with $\boldsymbol{\mu}_{\text{prior}} = \mathbf{0}$ and $\Sigma_{\text{prior}} = \mathbf{I}$. The reference field $\nu(\mathbf{x}; \boldsymbol{\mu}^*)$ and the solution of the inverse problem $\nu(\mathbf{x}; \hat{\boldsymbol{\mu}}_h)$ obtained with the full-order EnKF with $N_e = 500$ are represented in Fig. 10.

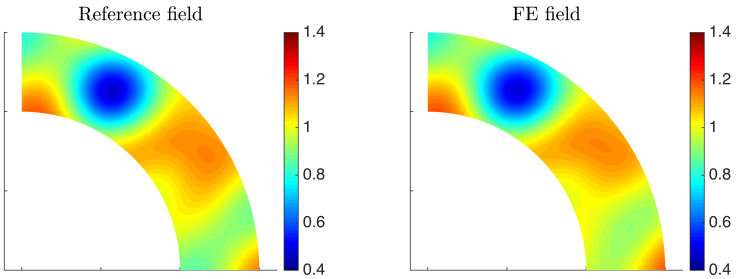

Figure 10: Reference (left) and estimated (right) field using the full-order EnKF.

In this case, the estimation problem is even more challenging than in the test case 1: the state/parameter estimation problem solution with the full-order EnKF requires more than 38 hours of CPU time and constructing the ROM is very expensive due to the higher dimension of the parameter space and the complex nonlinear dynamics. The REM allows a satisfying trade off between performance and accuracy. We compare the results obtained by solving the state/parameter estimation problem when relying on a reduced EnKF taking $m_D = 300$ DEIM elements, $n = [115, 150, 185]$ basis functions and by considering a REM built upon a calibration sample $S_{cal} = S_{train}$ of dimension $N_{train} = 420$. As shown in Fig. 11, the uncorrected RB-EnKF fails in the estimation of the unknown field for $n = [115, 150]$, that is, if the RB approximation is too coarse. For each choice of n, we recover more accurate reconstructions of the field using the corrected RB-EnKF with respect to the uncorrected procedure (the error $|\nu(\mathbf{x}; \hat{\boldsymbol{\mu}}_c) - \nu(\mathbf{x}; \hat{\boldsymbol{\mu}}_h)|$ is reduced by at least an order of magnitude with respect to $|\nu(\mathbf{x}; \hat{\boldsymbol{\mu}}_n) - \nu(\mathbf{x}; \hat{\boldsymbol{\mu}}_h)|$, without extra-costs due to the calibration procedure.

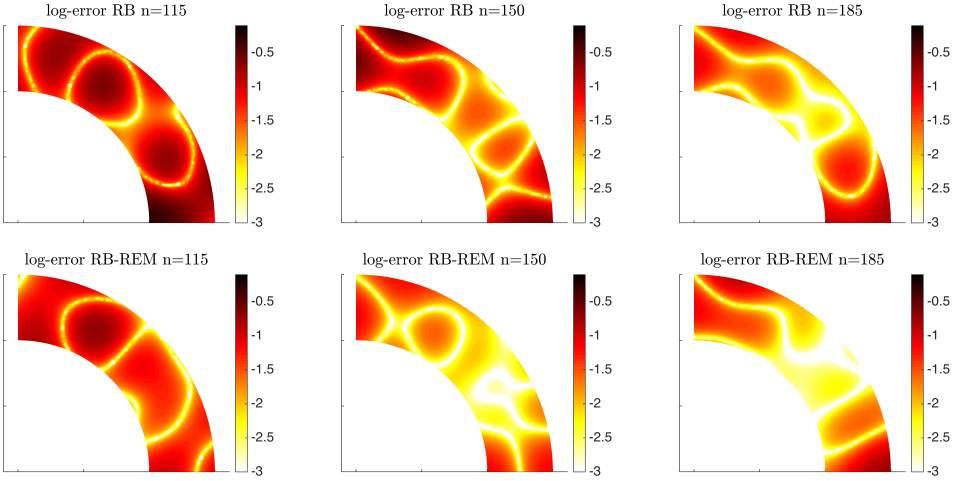

Figure 11: Errors between reference and estimated fields for different RB dimensions $n = 115, 150, 185$, without (top) and with (bottom) REM correction. This latter clearly yields a relevant improvement in the estimated field.

As shown in Table 4, the ROM construction requires several hours to be performed, but the online costs of the reduced EnKF are considerably smaller with respect to those obtained using the full-order EnKF. The negligible extra costs of the corrected RB-EnKF, togheter with the improved accuracy in the estimation, clearly motivate the introduction of a REM in the solution of complex state/parameter estimation problems.

	RB			FE
	$n = 115$	$n = 150$	$n = 185$	$N_h = 2768$
dof reduction	95.8%	94.5%	93.3%	0%
Forward solution	2.7 s	3.9 s	5 s	279 s
$\lvert S_{train}\rvert = 420$				
ROM contruction	31 h	31 h	31 h	
State/parameter estimation problem				
EnKF time	25 m	34 m	46 m	38 h 50 m
EnKF REM $N_{cal} = 420$	54 m	62 m	76 m	

Table 4: Test case 2: computational performances of the estimation procedure (offline construction and online inversion stages) and comparison with the FOM case.

We finally point out that developing efficient ROMs for problems involving traveling fronts is still an open issue; we remark that the proposed framework to solve Bayesian inverse and data assimilation problems is rather general and can be integrated within any choice of surrogate or reduced-order models.

7 Conclusions

The RB-EnKF approach proposed in this paper allows to speed up the solution of state/parameter estimation problems without affecting the accuracy of the computed estimates. Since the EnKF requires repetitive evaluations of solutions (and outputs) of the nonlinear dynamical system, in order to reduce the cost of the inversion procedure we can replace the forward map $\boldsymbol{\mu} \to \mathbf{s}_h(t;\boldsymbol{\mu})$ with the less expensive one $\boldsymbol{\mu} \to \mathbf{s}_n(t;\boldsymbol{\mu})$ obtained using a RB method instead of a full-order model. Our numerical results confirm that a considerable speedup is achieved when using the RB-EnKF instead of the full-order EnKF: the computational speedup in performing the filter goes from $55\times$ to $64.5\times$ for the first test case and from $50\times$ to $93\times$ in the second one. Nevertheless, the propagation of the reduction errors during the inversion procedure leads to biased estimates of the unknown state/parameter, as underlined also by our error analysis. The RB-EnKF has to be equipped with a statistical REM in order to recover unbiased output evaluation and consequently to guarantee the accuracy of the overall filtering technique. Moreover, the additional costs introduced by the REM are negligible: in the worst case scenario the computational time required by the corrected RB-EnKF is twice the uncorrected RB-EnKF, ensuring anyway a considerable speed up with respect to the use of a full-order EnKF.

References

[1] J. L. Anderson and S. L. Anderson, *A Monte Carlo implementation of the nonlinear filtering problem to produce ensemble assimilations and forecasts*, Monthly Weather Review, 127 (1999), pp. 2741–2758.

[2] P. Benner, S. Gugercin, and K. Willcox, *A survey of projection-based model reduction methods for parametric dynamical systems*, SIAM Review, 57 (2015), pp. 483–531.

[3] C. Brett, K. F. Lam, K. Law, D. McCormick, M. Scott, and A. Stuart, *Accuracy and stability of filters for dissipative pdes*, Physica D: Nonlinear Phenomena, 245 (2013), pp. 34–45.

[4] S. Chaturantabut and D. C. Sorensen, *Nonlinear model reduction via discrete empirical interpolation*, SIAM J. Sci. Comp., 32 (2010), pp. 2737–2764.

[5] N. Cressie, *Fitting variogram models by weighted least squares*, Journal of the International Association for Mathematical Geology, 17 (1985), pp. 563–586.

[6] T. Cui, Y. M. Marzouk, and K. E. Willcox, *Data-driven model reduction for the Bayesian solution of inverse problems*, International Journal for Numerical Methods in Engineering, 102 (2015), pp. 966–990.

[7] M. Dihlmann and B. Haasdonk, *A reduced basis kalman filter for parametrized partial differential equations*, ESAIM: COCV, 22 (2016), pp. 625–669.

[8] A. Doucet, S. Godsill, and C. Andrieu, *On sequential monte carlo sampling methods for bayesian filtering*, Statistics and computing, 10 (2000), pp. 197–208.

[9] M. Drohmann and K. Carlberg, *The ROMES method for statistical modeling of reduced-order-model error*, SIAM/ASA Journal on Uncertainty Quantification, 3 (2015), pp. 116–145.

[10] O. G. Ernst, B. Sprungk, and H.-J. Starkloff, *Bayesian inverse problems and Kalman filters*, in Extraction of Quantifiable Information from Complex Systems, vol. 102 of Lecture Notes in Computational Science and Engineering, Springer International Publishing, 2014, pp. 133–159.

[11] G. Evensen, *The ensemble Kalman filter: Theoretical formulation and practical implementation*, Ocean dynamics, 53 (2003), pp. 343–367.

[12] G. Evensen, *Data assimilation: the ensemble Kalman filter*, Springer Science & Business Media, 2009.

[13] R. FitzHugh, *Impulses and physiological states in theoretical models of nerve membrane*, Biophysical journal, 1 (1961), p. 445.

[14] M. Frangos, Y. Marzouk, K. Willcox, and B. van Bloemen Waanders, *Surrogate and reduced-order modeling: A comparison of approaches for large-scale statistical inverse problems*, Large-Scale Inverse Problems and Quantification of Uncertainty, 123149 (2010).

[15] D. Galbally, K. Fidkowski, K. Willcox, and O. Ghattas, *Non-linear model reduction for uncertainty quantification in large-scale inverse problems*, International journal for numerical methods in engineering, 81 (2010), pp. 1581–1608.

[16] R. Giraldo, P. Delicado, and J. Mateu, *Ordinary kriging for function-valued spatial data*, Environmental and Ecological Statistics, 18 (2011), pp. 411–426.

[17] G. H. Golub and C. F. Van Loan, *Matrix computations*, vol. 3, JHU Press, 2012.

[18] G. A. Gottwald and J. Harlim, *The role of additive and multiplicative noise in filtering complex dynamical systems*, in Proc. R. Soc. A, vol. 469, The Royal Society, 2013.

[19] T. M. Hamill, *Ensemble-based atmospheric data assimilation*, vol. Predictability of Weather and Climate, Cambridge Press, 2006, ch. 6, pp. 124–156.

[20] C. Himpe and M. Ohlberger, *Data-driven combined state and parameter reduction for inverse problems*, Advances in Computational Mathematics, 41 (2015), pp. 1343–1364.

[21] P. Houtekamer and F. Zhang, *Review of the ensemble Kalman filter for atmospheric data assimilation*, Monthly Weather Review, 144 (2016), pp. 4489–4532.

[22] J. Huttunen and J. Kaipio, *Approximation error analysis in nonlinear state estimation with an application to state-space identification*, Inverse Problems, 23 (2007), p. 2141.

[23] M. A. Iglesias, K. J. Law, and A. M. Stuart, *Ensemble Kalman methods for inverse problems*, Inverse Problems, 29 (2013), p. 045001.

[24] J. Kaipio and E. Somersalo, *Statistical and computational inverse problems*, vol. 160, Springer Science & Business Media, 2006.

[25] K. Law, A. Stuart, and K. Zygalakis, *Data Assimilation: A Mathematical Introduction*, Texts in Applied Mathematics, Springer International Publishing, 2015.

[26] Y. Maday, N. C. Nguyen, A. T. Patera, and S. H. Pau, *A general multipurpose interpolation procedure: the magic points*, Communications on Pure and Applied Analysis, 8 (2009), pp. 383–404.

[27] A. Manzoni, S. Pagani, and T. Lassila, *Accurate solution of Bayesian inverse uncertainty quantification problems combining reduced basis methods and reduction error models*, SIAM/ASA J. Uncertainty Quantification, 4 (2016), pp. 380–412.

[28] A. Menafoglio, P. Secchi, and M. Dalla Rosa, *A universal kriging predictor for spatially dependent functional data of a Hilbert space*, Electronic Journal of Statistics, 7 (2013), pp. 2209–2240.

[29] H. L. Mitchell, P. L. Houtekamer, and G. Pellerin, *Ensemble size, balance, and model-error representation in an ensemble Kalman filter*, Monthly Weather Review, 130 (2002), pp. 2791–2808.

[30] F. Negri, A. Manzoni, and D. Amsallem, *Efficient model reduction of parametrized systems by matrix discrete empirical interpolation*, Journal of Computational Physics, 303 (2015), pp. 431–454.

[31] A. Quarteroni, A. Manzoni, and F. Negri, *Reduced Basis Methods for Partial Differential Equations. An Introduction*, vol. 92 of Unitext Series, Springer International Publishing, 2016.

[32] A. Solonen, T. Cui, J. Hakkarainen, and Y. Marzouk, *On dimension reduction in Gaussian filters*, arXiv preprint arXiv:1508.06452, (2015).

[33] R. Ştefănescu and A. Sandu, *Efficient approximation of sparse jacobians for time-implicit reduced order models*, arXiv:1409.5506v3, (2015).

[34] A. M. Stuart, *Inverse problems: a Bayesian perspective*, Acta Numerica, 19 (2010), pp. 451–559.

[35] A. Tarantola, *Inverse problem theory and methods for model parameter estimation: SIAM*, 2005.

[36] V. Tikhomirov, *A study of the diffusion equation with increase in the amount of substance, and its application to a biological problem*, in Selected works of AN Kolmogorov, Springer, 1991.

A Construction of a functional kriging interpolant

Assume that the error $\{\chi_t(\boldsymbol{\mu}),\ \boldsymbol{\mu} \in \mathcal{P}\}$ is a (functional) random field, that is, a set of (functional) random variables indexed by $\boldsymbol{\mu} \in \mathcal{P}$, taking values in $L^2(a,b)$, with $(a,b) \subseteq (0,T)$. We assume that $\chi_t(\boldsymbol{\mu})$ is a second-order stationary and isotropic random process, that is:

1. the mean and the variance are constant with respect to $\boldsymbol{\mu} \in \mathcal{P}$, i.e.

$$\mathbb{E}[\chi_t(\boldsymbol{\mu})] = m_\chi(t), \qquad Var[\chi_t(\boldsymbol{\mu})] = \sigma^2_\chi(t), \qquad t \in (a,b);$$

2. the covariance depends only on the lag $\delta = \|\boldsymbol{\mu}_\alpha - \boldsymbol{\mu}_\beta\|$, i.e.

$$Cov(\chi_{t_1}(\boldsymbol{\mu}_\alpha), \chi_{t_2}(\boldsymbol{\mu}_\beta)) = c_{t_1,t_2}(\boldsymbol{\mu}_\alpha, \boldsymbol{\mu}_\beta) = c_{t_1,t_2}(\delta), \qquad \boldsymbol{\mu}_\alpha, \boldsymbol{\mu}_\beta \in \mathcal{P}, \quad t_1, t_2 \in (a,b);$$

   moreover, if $t_1 = t_2 = t$, we denote by $c_t(\delta) = c_{t_1,t_2}(\delta)$.

Given a sample of known functions of the random process $\{\chi_t(\boldsymbol{\mu}_q)\}_{q=1}^{N_{cal}}$, the best linear unbiased predictor (BLUP) of $\{\chi_t(\boldsymbol{\mu}_0)\}$, for each new $\boldsymbol{\mu}_0 \in \mathcal{P}$, is given by the linear combination

$$\hat{\chi}_t(\boldsymbol{\mu}) = \sum_{q=1}^{N_{cal}} \lambda_q(\boldsymbol{\mu}) \chi_t(\boldsymbol{\mu}_q) \qquad \forall \boldsymbol{\mu} \in \mathcal{P}$$

whose weights are obtained by imposing that the mean square error of $\hat{\chi}_t(\boldsymbol{\mu}_0)$ is minimized,

$$[\lambda_1(\boldsymbol{\mu}_0), \ldots, \lambda_{N_{cal}}(\boldsymbol{\mu}_0)]^T = \arg \min_{\lambda_1,\ldots,\lambda_{N_{cal}}} \int_a^b Var\left[\hat{\chi}_t(\boldsymbol{\mu}_0) - \chi_t(\boldsymbol{\mu}_0)\right] dt \tag{39}$$

under the constraint that $\hat{\chi}_t(\boldsymbol{\mu}_0)$ is unbiased,

$$\mathbb{E}[\hat{\chi}_t(\boldsymbol{\mu}_0) - \chi_t(\boldsymbol{\mu}_0)] = 0. \tag{40}$$

Finding the BLUP yields a constrained quadratic programming problem (for each $\boldsymbol{\mu}_0$): indeed,

$$Var(\hat{\chi}_t(\boldsymbol{\mu}_0) - \chi_t(\boldsymbol{\mu}_0)) = \sum_{q,p=1}^{N_{cal}} \lambda_q(\boldsymbol{\mu}_0)\lambda_p(\boldsymbol{\mu}_0) c_t(\boldsymbol{\mu}_q, \boldsymbol{\mu}_p) + c_t(\boldsymbol{\mu}_0, \boldsymbol{\mu}_0) - 2\sum_{q=1}^{N_{cal}} \lambda_q(\boldsymbol{\mu}_0) c_t(\boldsymbol{\mu}_i, \boldsymbol{\mu}_0), \tag{41}$$

$$\mathbb{E}[\hat{\chi}_t(\boldsymbol{\mu}_0) - \chi_t(\boldsymbol{\mu}_0)] = \sum_{q=1}^{N_{cal}} \lambda_q(\boldsymbol{\mu}_0)\mathbb{E}[\hat{\chi}_t(\boldsymbol{\mu}_q)] - \mathbb{E}[\hat{\chi}_t(\boldsymbol{\mu}_0)] = \mathbb{E}[\hat{\chi}_t(\boldsymbol{\mu}_0)](\sum_{q=1}^{N_{cal}} \lambda_q(\boldsymbol{\mu}_0) - 1),$$

thanks to assumption 1. Denoting by

$$\mathcal{L}(\lambda_1, \ldots, \lambda_{N_{cal}}, \eta) = \int_a^b Var(\hat{\chi}_t(\boldsymbol{\mu}_0) - \chi_t(\boldsymbol{\mu}_0))dt + \eta \int_a^b \mathbb{E}[\hat{\chi}_t(\boldsymbol{\mu}_0)dt - \chi_t(\boldsymbol{\mu}_0)]$$

the Lagrangian functional associated to problem (39)–(40), from the first-order necessary optimality conditions, we get the following linear system to be solved, for each $\boldsymbol{\mu}_0$:

$$\begin{bmatrix} \int_a^b c_t(\boldsymbol{\mu}_1,\boldsymbol{\mu}_1)dt & \dots & \int_a^b c_t(\boldsymbol{\mu}_1,\boldsymbol{\mu}_{N_{cal}})dt & 1 \\ \vdots & \ddots & \vdots & \vdots \\ \int_a^b c_t(\boldsymbol{\mu}_{N_{cal}},\boldsymbol{\mu}_1)dt & \dots & \int_a^b c_t(\boldsymbol{\mu}_{N_{cal}},\boldsymbol{\mu}_{N_{cal}})dt & 1 \\ 1 & \dots & 1 & 0 \end{bmatrix} \begin{bmatrix} \lambda_1 \\ \vdots \\ \lambda_{N_{cal}} \\ \eta \end{bmatrix} = \begin{bmatrix} \int_a^b c_t(\boldsymbol{\mu}_i,\boldsymbol{\mu}_0)dt \\ \vdots \\ \int_a^b c_t(\boldsymbol{\mu}_{N_{cal}},\boldsymbol{\mu}_0)dt \\ 1 \end{bmatrix}.$$

Thanks to assumption 2, $c_t(\boldsymbol{\mu}_q,\boldsymbol{\mu}_p) = Cov(\chi_t(\boldsymbol{\mu}_q),\chi_t(\boldsymbol{\mu}_p)) = c_t(\|\boldsymbol{\mu}_q - \boldsymbol{\mu}_p\|)$ so that, by denoting $\gamma_t(\delta) = c_t(0) - c_t(\delta)$, the previous linear system can be equivalently rewritten as:

$$\begin{bmatrix} \int_a^b \gamma_t(0)dt & \dots & \int_a^b \gamma_t(\|\boldsymbol{\mu}_1 - \boldsymbol{\mu}_{N_{cal}}\|)dt & 1 \\ \vdots & \ddots & \vdots & \vdots \\ \int_a^b \gamma_t(\|\boldsymbol{\mu}_{N_{cal}} - \boldsymbol{\mu}_1\|)dt & \dots & \int_a^b \gamma_t(\|\boldsymbol{\mu}_{N_{cal}} - \boldsymbol{\mu}_{N_{cal}}\|)dt & 1 \\ 1 & \dots & 1 & 0 \end{bmatrix} \begin{bmatrix} \lambda_1 \\ \vdots \\ \lambda_{N_{cal}} \\ \eta \end{bmatrix} = \begin{bmatrix} \int_a^b \gamma_t(\|\boldsymbol{\mu}_i - \boldsymbol{\mu}_0\|)dt \\ \vdots \\ \int_a^b \gamma_t(\|\boldsymbol{\mu}_{N_{cal}} - \boldsymbol{\mu}_0\|)dt \\ 1 \end{bmatrix}. \tag{42}$$

To compute the components appearing in the matrix and the vector of system (42), we estimate the so-called *(theoretical) semi-variogram*

$$\gamma(\delta) = \int_a^b \gamma_t(\delta)dt$$

with an empirical semi-variogram

$$\hat{\gamma}(\delta) = \frac{1}{2|N(\delta)|} \sum_{i,j \in N(\delta)} \int_a^b (\chi_t(\boldsymbol{\mu}_i) - \chi_t(\boldsymbol{\mu}_j))^2 dt, \tag{43}$$

where $N(\delta) = \{(\boldsymbol{\mu}_i,\boldsymbol{\mu}_j) : \|\boldsymbol{\mu}_i - \boldsymbol{\mu}_j\| = \delta\}$. In practice, the empirical semi-variogram is estimated at M discrete points $\{\delta_1,\dots,\delta_M\}$. Through the estimated values $\{\hat{\gamma}(\delta_1),\dots,\hat{\gamma}(\delta_M)\}$, a parametric semi-variogram model (e.g. spherical, exponential or gaussian) is fitted using a least-squares approach [5]. In this paper we consider the spherical parametric semi-variogram

$$\gamma(\delta) = \begin{cases} d\left(1.5\frac{\delta}{c} - 0.5\left(\frac{\delta}{c}\right)^3\right) & \delta \le c \\ d & \delta > c \end{cases} \tag{44}$$

where c, d are identified by fitting (44) on the dataset $\{(\delta_m, \hat{\gamma}(\delta_m))\}_{m=1}^M$. Finally, we define the prediction trace-variance $\hat{\sigma}^2_\chi(\boldsymbol{\mu}_0)$ of the functional ordinary kriging as

$$\hat{\sigma}^2_\chi(\boldsymbol{\mu}_0) = \int_a^b Var(\hat{\chi}_t(\boldsymbol{\mu}_0) - \chi_t(\boldsymbol{\mu}_0))dt.$$

Using (41), we get

$$\hat{\sigma}^2_\chi(\boldsymbol{\mu}_0) = \int_a^b \left(\sum_{q,p=1}^{N_{cal}} \lambda_q(\boldsymbol{\mu}_0)\lambda_p(\boldsymbol{\mu}_0)c_t(\boldsymbol{\mu}_q,\boldsymbol{\mu}_p) + c_t(\boldsymbol{\mu}_0,\boldsymbol{\mu}_0) - 2\sum_{q=1}^{N_{cal}} \lambda_q(\boldsymbol{\mu}_0)c_t(\boldsymbol{\mu}_i,\boldsymbol{\mu}_0) \right) dt. \tag{45}$$

Since $\{\lambda_p(\boldsymbol{\mu}_0)\}_{p=1}^{N_{cal}}$ and η are the solution of the linear system (42), it holds

$$\int_a^b \left(\sum_{p=1}^{N_{cal}} \lambda_p(\boldsymbol{\mu}_0)c_t(\boldsymbol{\mu}_p,\boldsymbol{\mu}_q) \right) dt = \int_a^b c_t(\boldsymbol{\mu}_q,\boldsymbol{\mu}_0)dt - \eta \qquad \forall q = 1,\dots,N_{cal},$$

so that, by substituting this latter relation in (41), we finally get

$$\hat{\sigma}^2_\chi(\boldsymbol{\mu}_0) = \int_a^b \left(\sum_{q=1}^{N_{cal}} \lambda_q(\boldsymbol{\mu}_0)(c_t(\boldsymbol{\mu}_q,\boldsymbol{\mu}_0) + c_t(\boldsymbol{\mu}_0,\boldsymbol{\mu}_0)) - 2\sum_{q=1}^{N_{cal}} \lambda_q(\boldsymbol{\mu}_0) c_t(\boldsymbol{\mu}_q,\boldsymbol{\mu}_0) \right) dt - \underbrace{\sum_{q=1}^{N_{cal}} \lambda_q(\boldsymbol{\mu}_0)}_{=1} \eta$$

$$= \int_a^b \left(\sum_{q=1}^{N_{cal}} \lambda_q(\boldsymbol{\mu}_0) \underbrace{(c_t(\boldsymbol{\mu}_0,\boldsymbol{\mu}_0) - c_t(\boldsymbol{\mu}_q,\boldsymbol{\mu}_0))}_{=\gamma_t(\|\boldsymbol{\mu}_q - \boldsymbol{\mu}_0\|)} \right) dt - \eta = \sum_{q=1}^{N_{cal}} \lambda_q(\boldsymbol{\mu}_0)\gamma(\|\boldsymbol{\mu}_q - \boldsymbol{\mu}_0\|) - \eta. \tag{46}$$

B Test case 1: further analysis

Referring to the test case 1 of Section 6.1, we first compare the outcome of the full-order EnKF algorithm in the case where different prior distributions and true parameter vectors are chosen. With respect to the results reported in Figure 3, obtained with

$$\boldsymbol{\mu}_{\text{prior}} = [0.7, 0.07, 0.76]^T, \qquad \Sigma_{\text{prior}} = \text{diag}([4\cdot 10^{-4}, 9\cdot 10^{-5}, 4\cdot 10^{-3}]^T),$$

and $\boldsymbol{\mu}^* = [0.6331, 0.0985, 0.7197]^T$, we consider the following test cases:

1. additional problem 1:

$$\boldsymbol{\mu}_{\text{prior}} = [0.66, 0.07, 0.9]^T, \qquad \boldsymbol{\mu}^* = [0.6202, 0.1259, 0.4131]^T,$$

2. additional problem 2:

$$\boldsymbol{\mu}_{\text{prior}} = [0.53, 0.113, 0.33]^T, \qquad \boldsymbol{\mu}^* = [0.6777, 0.0647, 0.5610]^T.$$

We solve these two additional state/parameter estimation problems by using the *full-order* EnKF (see Fig. 12) in order to analyze the convergence of the algorithm when different data are considered. When the mean of the prior distribution on $\boldsymbol{\mu}$ is less close to the *true* value $\boldsymbol{\mu}^*$, the EnKF algorithm still converges to $\boldsymbol{\mu}^*$, however requiring more iterations to produce estimates that are close to $\boldsymbol{\mu}^*$; compare, e.g., the trend of the estimate $(\hat{\boldsymbol{\mu}}_h)_3$ in the figure below with the corresponding case of Figure 3.

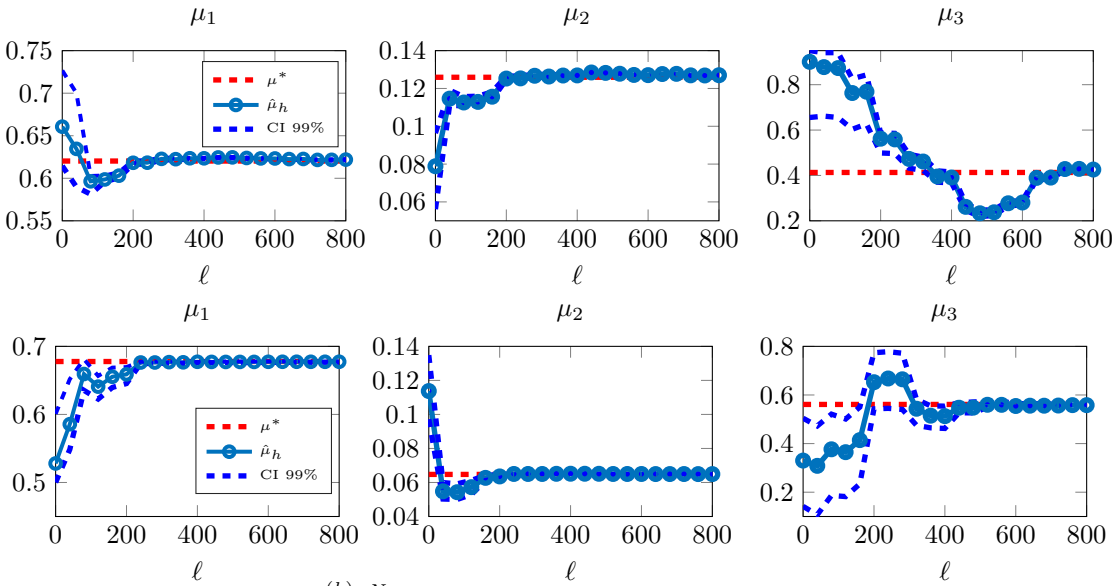

Figure 12: $\boldsymbol{\mu}^*$ versus $\{\hat{\boldsymbol{\mu}}_h^{(k)}\}_{k=1}^{N_\tau}$ for different initial ensembles using $N_e = 100$ particles.

Then, we turn to the comparison between the RB-EnKF algorithm and its corrected version, in order to assess the effect of the proposed REM in reducing the bias in the parameter estimation as a function of the noise variance σ.

In the case $\sigma = 5\sigma_0$ (first row of Fig. 13), the results of the RB-EnKF for $n = 15$ are comparable with the ones of the full-order EnKF, meaning that the reduction error is negligible with respect to the noise. This is not true when the RB dimension is set to $n = 7, 11$. In these two cases, there is a bias in the first two components of the parameter vector estimate. On the other hand, for a lower noise variance, such as in the case $\sigma = \sigma_0$ (second row of Fig. 13), we observe that the reduction error affects the parameter estimate for all RB dimensions $n = 7, 11, 15$.

For both values of the noise variance, the REM is therefore essential to improve the accuracy of the RB-EnKF estimates: as a matter of fact, the proposed REM based on curve kriging improves (by minimizing the propagation of the reduction error) the parameter estimation in our RB-EnKF up to two orders of magnitude in some cases; compare, e.g. Fig. 13 with Fig. 14.

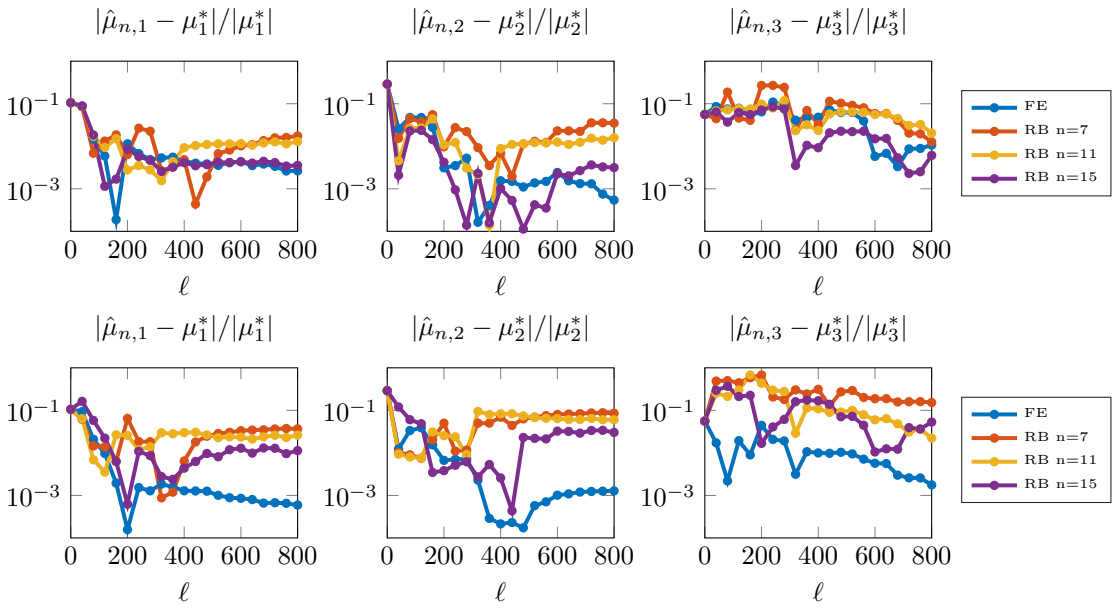

Figure 13: Relative error on estimated parameter components $|\mu^* - \hat{\mu}_n^{(k)}|/|\mu^*|$ versus the RB dimension n for the RB-EnKF when different noise variances $\sigma = 5\sigma_0$ (first row) and $\sigma = \sigma_0$ (second row) are considered.

C Derivation of the Kalman update formula

In this section we provide the detailed derivation of the Kalman update formula (15) for the *analysis stage*. We will extend to our state/parameter case the derivation proposed for the state filter in [25, Chapter 4]. For simplicity we show the derivation procedure for the output

$$\mathbf{s}_h^{(k+1)}(\boldsymbol{\mu}) = \mathbf{H}\mathbf{u}_h^{(k+1)}(\boldsymbol{\mu}),$$

the more general case of (6) being essentially very similar to deal with. By assuming that the *prior* and the *likelihood* are multivariate Gaussian distributions, we can rewrite (10) for each element of the ensemble as

$$\begin{aligned} &\exp\left(-\frac{1}{2}\left\|\begin{bmatrix}\boldsymbol{\mu}\\ \mathbf{u}\end{bmatrix} - \begin{bmatrix}\boldsymbol{\mu}_q^{(k+1)}\\ \mathbf{u}_h^{(k+1)}(\boldsymbol{\mu}_q^{(k+1)})\end{bmatrix}\right\|_{\mathcal{C}^h}^2\right) \\ &\qquad \propto \exp\left(-\frac{1}{2}\left\|\mathbf{s}^{(k+1)} - \mathbf{s}_h^{(k+1)}(\boldsymbol{\mu})\right\|_{\mathbf{r}}^2 - \frac{1}{2}\left\|\begin{bmatrix}\boldsymbol{\mu}\\ \mathbf{u}\end{bmatrix} - \begin{bmatrix}\boldsymbol{\mu}_q^{(k)}\\ \mathbf{u}_h^{(k+1)}(\boldsymbol{\mu}_q^{(k)})\end{bmatrix}\right\|_{\mathcal{C}^h_{\text{prior}}}^2\right) \end{aligned} \tag{47}$$

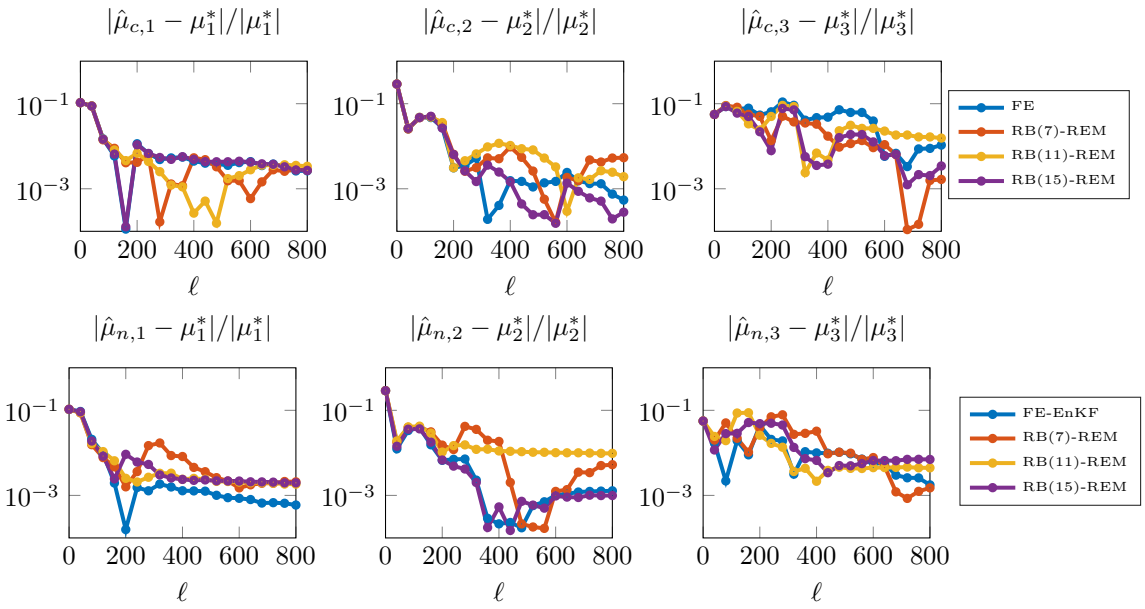

Figure 14: Relative error on estimated parameter components $|\mu^* - \hat{\mu}_n^{(k)}|/|\mu^*|$ versus the RB dimension n for the corrected RB-EnKF when different noise variances $\sigma = 5\sigma_0$ (first row) and $\sigma = \sigma_0$ (second row) are considered.

where $\mathcal{C}^h_{\text{prior}}$ is the covariance matrix of the parameter-state vector, given by

$$\mathcal{C}^h_{\text{prior}} = \begin{bmatrix} \mathbf{C}^{(k+1)}_{\mu\mu} & \mathbf{C}^{(k+1)}_{\mu u_h} \\ \mathbf{C}^{(k+1)}_{u_h\mu} & \mathbf{C}^{(k+1)}_{u_h u_h} \end{bmatrix}.$$

We recall that, in order to solve the inverse problem, we need to identify the unknown posterior mean $[\boldsymbol{\mu}_q^{(k+1)}, \mathbf{u}_h^{(k+1)}(\boldsymbol{\mu}_q^{(k+1)})]^T$ and the unknown covariance $\mathcal{C}^h$ of the posterior pdf. By requiring that the means and the covariances of the quantities appearing in (47) are equal, we derive two equations to be satisfied by the unknown mean and covariance:

$$(\mathcal{C}^h)^{-1} = (\mathcal{C}^h_{\text{prior}})^{-1} + \begin{bmatrix} \mathbf{0} \\ \mathbf{H} \end{bmatrix} \Gamma^{-1} \begin{bmatrix} \mathbf{0} \\ \mathbf{H} \end{bmatrix}^T, \tag{48}$$

$$(\mathcal{C}^h)^{-1} \begin{bmatrix} \boldsymbol{\mu}_q^{(k+1)} \\ \mathbf{u}_h^{(k+1)}(\boldsymbol{\mu}_q^{(k+1)}) \end{bmatrix} = (\mathcal{C}^h_{\text{prior}})^{-1} \begin{bmatrix} \boldsymbol{\mu}_q^{(k)} \\ \mathbf{u}_h^{(k+1)}(\boldsymbol{\mu}_q^{(k)}) \end{bmatrix} + \begin{bmatrix} \mathbf{0} \\ \mathbf{H} \end{bmatrix} \Gamma^{-1} \mathbf{s}^{(k+1)}. \tag{49}$$

From (48), by applying the Woodbury matrix identity (see e.g. [25, Chapter 4]), we get

$$\mathcal{C}^h = \left(\mathcal{I} - \mathcal{C}^h_{\text{prior}} \begin{bmatrix} \mathbf{0} \\ \mathbf{H} \end{bmatrix} (\boldsymbol{\Gamma} + \mathbf{C}^{(k+1)}_{s_h s_h})^{-1} \begin{bmatrix} \mathbf{0} \\ \mathbf{H} \end{bmatrix}^T \right) \mathcal{C}^h_{\text{prior}};$$

substituting this last expression in (49) we obtain:

$$\begin{aligned} \begin{bmatrix} \boldsymbol{\mu}_q^{(k+1)} \\ \mathbf{u}_h^{(k+1)}(\boldsymbol{\mu}_q^{(k+1)}) \end{bmatrix} &= \mathcal{C}^h \left((\mathcal{C}^h_{\text{prior}})^{-1} \begin{bmatrix} \boldsymbol{\mu}_q^{(k)} \\ \mathbf{u}_h^{(k+1)}(\boldsymbol{\mu}_q^{(k)}) \end{bmatrix} + \begin{bmatrix} \mathbf{0} \\ \mathbf{H} \end{bmatrix} \Gamma^{-1} \mathbf{s}^{(k+1)} \right) \\ &= \left(\mathcal{I} - \mathcal{C}^h_{\text{prior}} \begin{bmatrix} \mathbf{0} \\ \mathbf{H} \end{bmatrix} (\boldsymbol{\Gamma} + \mathbf{C}^{(k+1)}_{s_h s_h})^{-1} \begin{bmatrix} \mathbf{0} \\ \mathbf{H} \end{bmatrix}^T \right) \begin{bmatrix} \boldsymbol{\mu}_q^{(k)} \\ \mathbf{u}_h^{(k+1)}(\boldsymbol{\mu}_q^{(k)}) \end{bmatrix} + \mathcal{C}^h \begin{bmatrix} \mathbf{0} \\ \mathbf{H} \end{bmatrix} \Gamma^{-1} \mathbf{s}^{(k+1)}. \end{aligned}$$

By observing that

$$\mathcal{C}^h \begin{bmatrix} \mathbf{0} \\ \mathbf{H} \end{bmatrix} \Gamma^{-1} \begin{bmatrix} \mathbf{0} \\ \mathbf{H} \end{bmatrix}^T = \mathcal{I} - \mathcal{C}^h (\mathcal{C}^h_{\text{prior}})^{-1} = \mathcal{C}^h_{\text{prior}} \begin{bmatrix} \mathbf{0} \\ \mathbf{H} \end{bmatrix} (\boldsymbol{\Gamma} + \mathbf{C}^{(k+1)}_{s_h s_h})^{-1} \begin{bmatrix} \mathbf{0} \\ \mathbf{H} \end{bmatrix}^T$$

and that

$$\mathbf{s}^{(k+1)} - \begin{bmatrix} \mathbf{0} \\ \mathbf{H} \end{bmatrix}^T \begin{bmatrix} \boldsymbol{\mu}_q^{(k)} \\ \mathbf{u}_h^{(k+1)}(\boldsymbol{\mu}_q^{(k)}) \end{bmatrix} = \mathbf{s}^{(k+1)} - \mathbf{s}_h^{(k+1)}(\boldsymbol{\mu}_q^{(k)}),$$

we easily obtain the system (15) for the Kalman update. The generalization of the updating formula to the case of a different output, like the one expressed by (6), can be obtained in a very similar way by considering as prior mean

$$\left[\boldsymbol{\mu}_q^{(k)} \quad \mathbf{u}_h(\tau^{(k+1)}; \boldsymbol{\mu}_q^{(k)}) \quad \cdots \quad \mathbf{u}_h(t^{(\ell)}; \boldsymbol{\mu}_q^{(k)}) \quad \cdots \quad \mathbf{u}_h(\tau^{(k)}; \boldsymbol{\mu}_q^{(k)})\right]^T,$$

and as output operator $\left[\mathbf{0} \quad \Delta t\omega_K\mathbf{H} \quad \cdots \quad \Delta t\omega_{K-1}\mathbf{H} \quad \cdots \quad \Delta t\omega_1\mathbf{H}\right]^T$, and following the same approach of the proof reported above.

Recent publications:

MATHEMATICS INSTITUTE OF COMPUTATIONAL SCIENCE AND ENGINEERING
Section of Mathematics

Ecole Polytechnique Fédérale (EPFL)

CH-1015 Lausanne

06.2016 M.G.C. NESTOLA, E. FAGGIANO, C. VERGARA, R.M. LANCELLOTTI, S. IPPOLITO, S. FILIPPI, A. QUARTERONI, R. SCROFANI :
Computational comparison of aortic root stresses in presence of stentless and stented aortic valve bio-prostheses

07.2016 M. LANGE, S. PALAMARA, T. LASSILA, C. VERGARA, A. QUARTERONI, A.F. FRANGI:
Improved hybrid/GPU algorithm for solving cardiac electrophysiology problems on Purkinje networks

08.2016 ALFIO QUARTERONI, ALESSANDRO VENEZIANI, CHRISTIAN VERGARA:
Geometric multiscale modeling of the cardiovascular system, between theory and practice

09.2016 ROCCO M. LANCELLOTTI, CHRISTIAN VERGARA, LORENZO VALDETTARO, SANJEEB BOSE, ALFIO QUARTERONI:
Large Eddy simulations for blood fluid-dynamics in real stenotic carotids

10.2016 PAOLO PACCIARINI, PAOLA GERVASIO, ALFIO QUARTERONI:
Spectral based discontinuous Galerkin reduced basis element method for parametrized Stokes problems

11.2016 ANDREA BARTEZZAGHI, LUCA DEDÈ, ALFIO QUARTERONI:
Isogeometric analysis of geometric partial differential equations

12.2016 ERNA BEGOVIĆ KOVAČ, DANIEL KRESSNER:
Structure-preserving low multilinear rank approximation of antisymmetric tensors

13.2016 DIANE GUIGNARD, FABIO NOBILE, MARCO PICASSO:
A posteriori error estimation for the steady Navier-Stokes equations in random *domains*

14.2016 MATTHIAS BOLTEN, KARSTEN KAHL, DANIEL KRESSNER, FRANCISCO MACEDO, SONJA SOKOLOVIĆ:
Multigrid methods combined with low-rank approximation for tensor structured Markov chains

15.2016 NICOLA GUGLIELMI, MUTTI-UR REHMAN, DANIEL KRESSNER:
A novel iterative method to approximate structured singular values

16.2016 YVON MADAY, ANDREA MANZONI, ALFIO QUARTERONI :
An online intrinsic stabilitzation strategy for the reduced basis approximation of parametrized advection-dominated

17.2016 ANDREA MANZONI, LUCA PONTI :
An adjoint-based method for the numerical approximation of shape optimization problems in presence of fluid-structure interaction

18.2016 NEW STEFANO PAGANI, ANDREA MANZONI, ALFIO QUARTERONI:
Efficient state/Parameter estimation in nonlinear unsteady PDEs by a reduced basis ensemble Kalman filter